Award Number: W81XWH-11-1-0516

TITLE: Targeted Approach to Overcoming Treatment Resistance in Advanced Prostate Cancer

PRINCIPAL INVESTIGATOR: Dr. Karin Scarpinato

CONTRACTING ORGANIZATION: Georgia Southern University
Statesboro, GA 30458-6724

REPORT DATE: September 2015

TYPE OF REPORT: Final Addendum

PREPARED FOR: U.S. Army Medical Research and Materiel Command
Fort Detrick, Maryland 21702-5012

REPORT DOCUMENTATION PAGE

Form Approved
OMB No. 0704-0188

1. REPORT DATE	2. REPORT TYPE	3. DATES COVERED
September 2015	Final Addendum	1Jul2014 - 30Jun2015

4. TITLE AND SUBTITLE
Targeted Approach to Overcoming Treatment Resistance in

Advanced Prostate Cancer

5a. CONTRACT NUMBER

5b. GRANT NUMBER
W81XWH-11-1-0516

5c. PROGRAM ELEMENT NUMBER

6. AUTHOR(S)

Dr. Karin Scarpinato
Georgia Southern University

E-Mail: kscarpinato@georgiasouthern.edu

5d. PROJECT NUMBER

5e. TASK NUMBER

5f. WORK UNIT NUMBER

7. PERFORMING ORGANIZATION NAME(S) AND ADDRESS(ES)

Georgia Southern University
P.O. Box 8044
Statesboro, GA 30461

8. PERFORMING ORGANIZATION REPORT NUMBER

9. SPONSORING / MONITORING AGENCY NAME(S) AND ADDRESS(ES)

U.S. Army Medical Research and Materiel Command
Fort Detrick, Maryland 21702-5012

10. SPONSOR/MONITOR'S ACRONYM(S)

11. SPONSOR/MONITOR'S REPORT NUMBER(S)

12. DISTRIBUTION / AVAILABILITY STATEMENT

Approved for Public Release; Distribution Unlimited

13. SUPPLEMENTARY NOTES

14. ABSTRACT

The purpose of this project is to determine if rescinnamine is effective against prostate cancer and treatment resistance. We determined that rescinnamine is less effective against prostate cancer than against other cancer types, making it less ideal to follow. In addition, the hypotensive activity of rescinnamine was dose-inhibitive in animal studies. We therefore pursued a combination of computational modeling, chemical synthesis and in vitro testing to identify analogs with higher efficacy and less toxicity. Initial results identified a small number of compounds, some of them entirely novel, that should be followed up on in subsequent studies.

15. SUBJECT TERMS
rescinnamine, computational modeling, novel compounds, chemotherapy, prostate

16. SECURITY CLASSIFICATION OF:			17. LIMITATION OF ABSTRACT	18. NUMBER OF PAGES	19a. NAME OF RESPONSIBLE PERSON
a. REPORT	b. ABSTRACT	c. THIS PAGE			USAMRMC
Unclassified	Unclassified	Unclassified	UU	41	19b. TELEPHONE NUMBER *(include area code)*

Table of Contents

Page

1. Introduction

This project explores new therapeutic approaches for advanced prostate tumors. This innovative approach engages computational modeling to identify compounds that target a specific, mismatch repair protein-dependent cell death pathway.
A previously identified compound, rescinnamine is being tested for its efficacy against prostate cancer, and subsequently further developed. Problems with the hypotensive activity of rescinnamine lead to the need to identify analogs that show efficacy in cell killing, while reducing side effects, as was outlined in the original proposal as "alternate approaches".

2. Keywords

Chemotherapy, prostate cancer, rescinnamine, analogs, computational modeling

3. Overall Project Summary

The purpose of this project is to determine if rescinnamine is effective against prostate cancer and treatment resistance. We determined that rescinnamine is less effective against prostate cancer than against other cancer types, making it less ideal to follow. In addition, the hypotensive activity of rescinnamine was dose-inhibitive in animal studies. We therefore pursued a combination of computational modeling, chemical synthesis and in vitro testing to identify analogs with higher efficacy and less toxicity. Initial results identified a small number of compounds, some of them entirely novel, that should be followed up on in subsequent studies.

4. Key Research Accomplishments

Results with rescinnamine in animals lead to problems with the hypotensive activity of the drug. We therefore went back to the computational modeling part to predict analogs that would show improved cell killing activity while reducing side effects. This approach was described in the "alternate approaches" section of the proposal. Furthermore, we have been adding basic experiments to understand the cell death initiation by rescinnamine and other compounds in the cell. A new rescinnamine analog was identified during these studies that shows higher efficacy than any of the other compounds tested, and in cell culture, functions against taxol-resistant prostate cancer cells.
A graduate student and several undergraduate students (as volunteers) have worked on the project.

Task 1: To demonstrate that a compound mimicking platinum-induced cell death effectively targets chemotherapy-resistant, androgen-independent prostate cancer cells

Task 1a. Growth of cell lines

All indicated cell lines (RWPE-1, PC-3, PC-3-T55, LNCaP) were grown in the laboratory after the new biohood was installed. Growth was somewhat delayed due to the installation. All cell lines have been successfully grown.

Task 1b. MTS assays with rescinnamine

All sensitive prostate cancer cell lines were tested against rescinnamine, as indicated in the SOW. We added an ovarian cancer cell line, A2780, as a positive control, which would provide induction of cell death and determine real results vs. technical problems.
RWPE-1 cells are immortalized prostatic epithelial cells. As seen in Fig. 1, rescinnamine induces some cell death, but at about 20 uM of rescinnamine, the effect levels off around 70% cell viability.

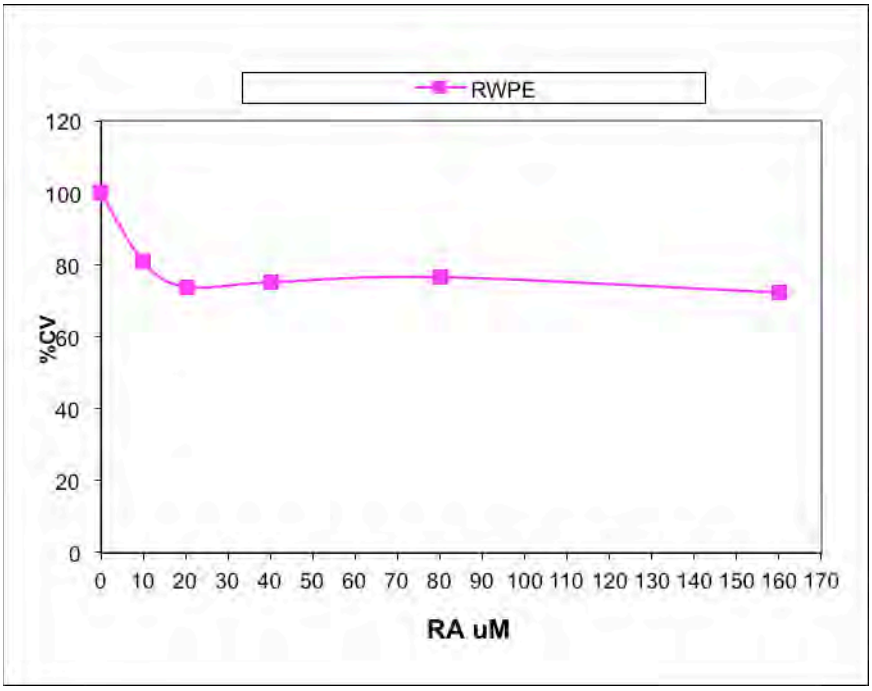

Fig. 1. Effect of increasing concentrations of rescinnamine (RA) on cell viability (CV) of RWPE-1, as determined in an MTS assay.

Previous results with other cell lines showed a similar drop at 20 uM that, however went to 0-20% cell viability. The main difference that we could identify to these experiments is that we now correct for the amount of solvent (acetic acid/DMSO) that was not done previously. This means that previous results simply added increasing amounts of solvent together with drug; cell viability then shows a combination of drug and solvent effect. In these new experiments, we are correcting for the amount of solvent as the drug concentration increases. To determine the exact solvent effect, we added A2780 cells with (eq) and without (not eq) correction for solvent. Based on these results, the solvent concentration causes a much stronger "dip" around 20 uM and plateaus off at an at least 10 % lower cell viability (Fig. 2).

We next determined the viability of LnCaP cells in the presence of rescinnamine (Fig. 2). Again, increasing concentrations plateau off around 70% cell viability, low concentration do not seem to effect cell growth at all.

The drug is therefore not very effective against "normal" prostatic cancer cells or androgen-responsive cells. However, LnCAP cells are deficient in MSH2. We previously determined that cell death induced by rescinnamine at least partially is dependent on functional MSH2. These results are in line with expectations that the drug will not function without MSH2, and is more specific for tumor cells.

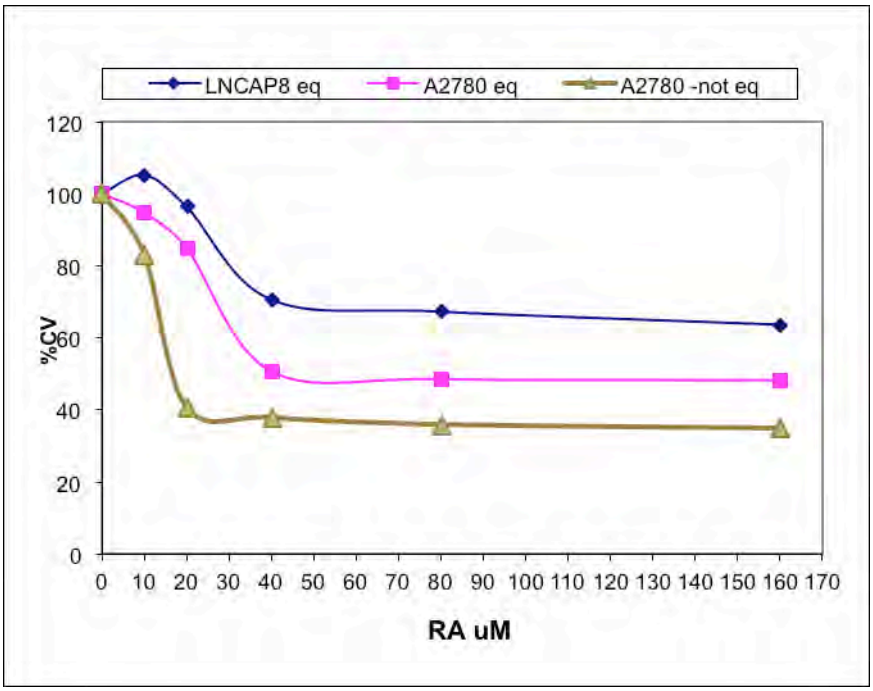

Fig. 3 compares the effect of rescinnamine on RWPE and LnCAP cells, with A2780 cells added as a control. Overall, the effect of rescinnamine on prostate cancer cells is much weaker than what we previously observed with other cell lines (Vasilyeva et al., 2009).

Fig. 2. Effect of increasing concentrations of rescinnamine (RA) on cell viability (CV) of LnCAP, as determined in an MTS assay. A2780: ovarian cancer cell lines, control; eq: solvent adjusted with increasing drug concentration; not eq: solvent concentration not adjusted

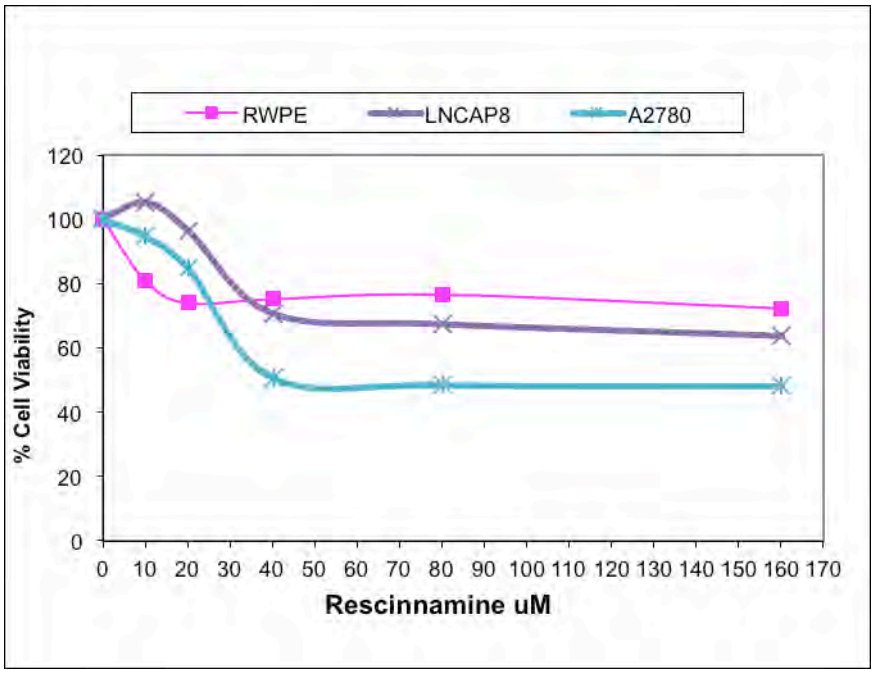

Fig. 3. Comparing the effect of increasing concentrations of rescinnamine on cell viability of RWPE and LnCAP cells. A2780 was added as a control.

We next determine the effect of the drug on PC3 cells, representing a hormone-independent cancer cell line. As shown in Fig. 4, increasing amounts of rescinnamine show a very gradual decline on cell viability of PC3 cells. These results need to be repeated.

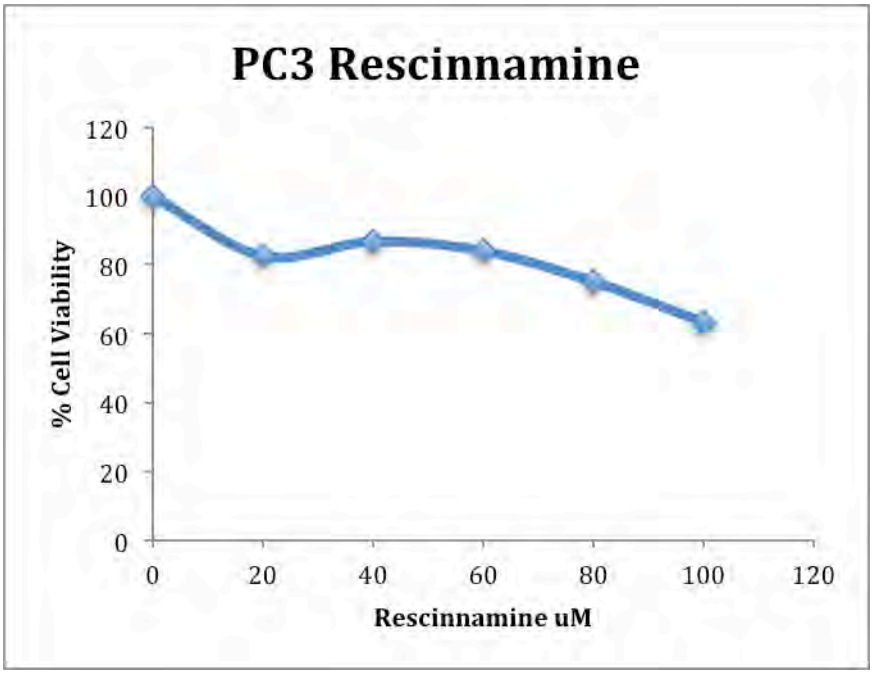

Fig. 4: Cell viability assay (MTS) with increasing amounts of rescinnamine and PC3 cells.

Rescinnamine therefore does not appear to be highly effective on prostate cancer cells, regardless of the presence/absence of MSH2 or hormone dependence.

Together with the result from the animal work, described below, we decided to follow through with the work described in the "Potential Pitfalls/Alternative Approaches" section, which describes the use of computational modeling to identify more potent rescinnamine derivatives.
We also since have ordered controlled cell lines from ATCC that have a known number of passages. Given that cancer cells are generally genetically unstable and each passage will add to the instability, we will continue with these cell lines upon their arrival.

As mentioned above, we went back to computational predictions, after rescinnamine showed adverse effects in the animal study, and as outlined in our anticipated results and pitfalls. Molecular docking experiments were performed as follows:
The molecular docking was performed in four phases; structural model generation, ligand library generation, receptor grid generation and finally docking of the ligand library into the receptor grid. Models for the structures were generated using molecular dynamics as in our previous works (Vasilyeva, A et al, 2009; Vasilyeva, A et al, 2010;Salsbury. 2010). However, for this work more extensive simulations were used. The details of these simulations are reported elsewhere (Negureanu and Salsbury, 2012). In short, the simulations were four 20ns NPT all-atom simulations based on the human MSH2/6 crystal structure (Morris et al, 2009), with the (1,2)G cross-link, which is the predominate damage due to cisplatin. The structure selected was the median structure of the most populated cluster found from all-atom RMSD-based clustering (Negureanu and Salsbury, 2012). The appropriate pdbqs file was generated with the DNA removed, so that just the protein remained, using defaults from Autodock4.
Libraries for docking were based on the core of the rescinnamine structure. All possible derivatives were made based on this structure, with R1, R2 and R3 selected from H, OH, COOH, NH_2, and OCH_3. Also, a structure without the modified phenyl ring was docked (Compound 1, Table I). The best of these compounds were suggested for chemical synthesis based on their synthetic accessiblity. We also explored larger libraries, and ones with other functional modifications, but these were not readily synthesized and not discussed herein. Autodock tools were used to generate 3D pdbq files with charges and the correct number of rotatable bonds.
The grids for docking were generated using Autodock4 with the grid centered at the position of the platinum atom in the full protein-DNA complex, however, the DNA was removed prior to grid generation. Cubic 22.5A grids were generated for electrostatics, and vdW parameters for C, S, O, N and polar H with a grid spacing of 0.375A.
The dockings were performed using Autodock4's defaults for it's Lamarckian Genetic Algorithm with a population size of 150, a maximum number of energy evaluations of 5 million and a maximum number of generations of 27000. Each derivative was subjected to 256 runs and ranked according to the best predicted Ki.

An organic chemist was included in this work who synthesized the predicted compounds. General chemistry is described as follows:
Reagents were obtained from commercial sources and used without additional purification. Extraction and flash chromatography solvents were technical grade. Flash chromatography was carried out using a Biotage SP1-B2A0/ HPFC System. Analytical thin layer chromatography (TLC) was performed on silica gel plates with C-4 Spectroline 254 indicator. Visualization was accomplished with UV light and 20% phosphomolybdic acid solution in EtOH. LC-MS, ESI-MS and HPLC solvents were HPLC grade. Melting points were determined on a Mel-Temp apparatus. ^{1}H NMR and $^{13}CNMR$ spectra were taken in commercial deuterated solvents and recorded on a Bruker Advance 300 MHz and Bruker DRX-500 spectrometer using a 5mm TBI probe equipped with z axis gradients. Probe temperature was regulated at 25° C. All data was collected and processed with Topspin 1.3 using standard Bruker processing parameters. Chemical shifts (δ) are given in ppm; multiplicities are indicated by s (singlet), d (doublet), t (triplet), q (quartet), m (multiplet), dd (doublet of doublet) and br (broad).
Acryloyl reserpate (1). Dry distilled pyridine (791mg, 0.808mL, 10mmole) was added to a mixture of methyl reserpate (300mg, 0.74mmole) and acryloyl chloride (135.77mg, 0.123mL, 1.5mmole) was added and stirred under nitrogen at room temperature for 74 hr. Excess pyridine was evaporated and the

residue was taken up in chloroform (50 mL) and the organic layer washed with water (3x 20 mL) and brine, the organic layer was dried with anhydrous Na_2SO_4, filtered and evaporated under reduced pressure to give a residue that was purified by flash chromatography (silica gel, chloroform/methanol, 3%, R_f 0.3) giving a solid rinsed with methanol to afford 1 (120 mg, 35%) as white crystals : mp >260 ^oC; ^1H-NMR (300 MHz, $CDCl_3$, δ): 7.80 (s, 1H), 7.31(d, 1H, J= 8.52 Hz), 6.81 (s, 1H, J= 1.95 Hz), 6.76 (d, 1H, J= 8.53 Hz), 6.45(d, 1H, J= 17.32 Hz), 6.15 (dd, 1H, J= 17.31& 17.30 Hz), 5.87 (d, 1H, J= 10.4 Hz), 4.90-4.82 (m, 1H), 4.42 (s, 1H), 3.82 (s, 3H), 3.80 (s, 3H), 3.48 (s, 3H), 3.19-3.14 (m, 2H), 3.02-2.98 (m, 1H), 2.69-2.60 (m, 2H), 2.49-2.39 (m,2 H), 2.26- 2.17 (m, 2H), 2.04-1.78 (m, 5H); ^{13}C-NMR (75 MHz, $CDCl_3$, δ): 172.77, 165.42, 156.10, 136.31, 130.79, 130.45, 128.63, 122.13, 118.45. 108.92, 107.92, 95.18, 77.69, 77.54, 60.68, 55.76, 53.68, 51.75, 51.72, 51.17, 48.96, 33.93, 32.25, 29.47, 24.17, 16.75; ESI-MS: m/z= 469.2 (M^+ + H); Anal. Calcd. for $C_{26}H_{32}N_2O_6.0.3H_2O$, C, 65.81; H, 6.94; N, 5.90. Found: C, 65.60; H, 6.83; N, 6.01.

General procedure for the synthesis of rescinnamine derivatives (2-7) A mixture of the aryl iodide (0.507 mmole), acryloyl reserpate (300 mg, 0.641 mmole), Et_3N (0.06 g, 0.09 mL, 0.645 mmol) and $Pd(OAc)_2$ (1.23 mg, 0.005mmole) in the presence of tri-o-tolylphosphine (4.5 mg, 0.021mmole) in acetonitrile (20 mL) was heated with stirring in a capped sealed glass tube under argon at 90^{o}C for 48hrs. After cooling, the solvent was removed under reduced pressure; the residue was dissolved in chloroform (30 mL) and washed with water (3x15 mL) and brine. The organic layer was dried with anhydrous sodium sulfate, filtered and evaporated under reduced pressure to give a residue that was purified by flash chromatography to afford a solid that was recrystallized as described below:

For 2: (R_1 = $COOCH_3$, R_2 = OCH_3): White crystals recrystallized from methanol, yield = 180 mg (44%), (chloroform/methanol 3%, R_f = 0.7), mp = 215-217 ^{o}C; ^1H NMR (500 MHz, $CDCl_3$, δ): 8.03 (s, 1H), 7.69 (s, 1H), 7.67-7.66 (m, 2H), 7.35 (d, 1H, J= 8.52), 7.02 (d, 1H, J= 8.77 Hz), 6.86 (s, 1H), 6.79 (d, 1H, J= 8.5 Hz), 6.40 (d, 1H, J= 15.98), 4.97-4.92 (m, 1H), 4.47 (s, 1H), 3.97 (s, 3H), 3.95 (s, 3H), 3.86(s, 3H), 3.84 (s, 3H), 3.54 (s, 3H), 3.19-3.18 (m, 2H), 3.06-3.03 (m, 1H), 2.69-2.66 (m, 1H), 2.52-2.45 (m, 3H), 2.30- 2.25 (m, 2H), 1.98-1.80 (m, 5H); ^{13}C NMR (125 MHz, $CDCl_3$, δ): 172.94, 166.41, 166.11, 160.58, 156.03, 143.66, 136.30, 133.49, 131.63, 130.43, 126.48, 122.05, 120.28, 118.55, 116.84, 112.34, 108.94, 107.85, 95.04, 65.93, 60.97, 56.26, 55.76, 53.69, 52.40, 51.76, 51.17, 48.92, 33.92, 32.25, 31.08, 29.62, 24.21, 16.75, 15.33; ESI-MS: m/z= 633.4 (M^+ + H); Anal. Calcd for $C_{35}H_{40}N_2O_9$: C, 66.44; H, 6.37; N, 4.43; Found: C, 66.16; H, 6.46; N, 4.41.

For 3 (R_1 = OCH_3, R_2 = COOH): Yellow crystals recrystallized from diethyl ether, yield = 150 mg (38%), (chloroform/methanol 8%, R_f = 0.1), mp = 228-230 ^{o}C; ^1H NMR (300 MHz, DMSO, δ): 10.62 (s, 1H), 7.70 (d, 1H, J= 15.97 Hz), 7.58 (d, 1H, J=7.83 Hz), 7.47 (s, 1H), 7.32 (d, 1H, J= 7.83 Hz), 7.24 (d, 1H, J= 8.55Hz), 6.82 (s, 1H), 6.79 (d, 1H, J= 15.91 Hz), 6.63 (d, 1H, J= 8.57 Hz), 4.90-4.82 (m, 1H), 4.53 (s, 1H), 3.88 (s, 3H), 3.79 (s, 3H), 3.75 (s, 3H), 3.43 (s, 3H), 3.17-3.11 (m, 3H), 2.97-2.84 (m, 3H), 2.72-2.66 (m, 1H), 2.24 (d, 1H), 1.87-1.73 (m, 6H); ^{13}C NMR (75 MHz, DMSO, δ): 171.81, 170.22, 165.82, 157.10, 155.80, 144.75, 137.20, 136.09, 129.43, 128.36, 121.26, 120.57, 118.97, 118.67, 111.83, 108.99, 105.82, 94.88, 79.40, 77.59, 76.63, 60.55, 55.99, 55.40, 53.47, 52.29, 50.73, 50.06, 48.87, 32.21, 31.29, 28.94, 23.05, 16.00; ESI-MS: m/z= 619.3 (M^+ + H); Anal. Calcd for $C_{34}H_{38}N_2O_9.2.5H_2O$: C, 61.53; H, 6.53; N: 4.22; Found: C, 61.41; H, 7.11; N, 4.00.

For 4 (R_1 = COOH, R_2 = OCH_3): Pale yellow solid recrystallized from diethyl ether, yield = 108 mg (27%), (chloroform/methanol 8%, R_f = 0.1), mp = 249-250 ^{o}C; ^1H NMR (500 MHz, DMSO, δ): 10.61 (s, 1H), 8.32 (s, 1H), 7.93 (s, 1H), 7.87 (d, 1H, J= 8.57 Hz), 7.70 (d, 1H, J= 15.96 Hz), 7.24 (d, 1H, J= 8.44 Hz), 7.16 (d, 1H, J= 8.66 Hz), 6.82 (s, 1H), 6.63 (d, 1H, J= 8.34 Hz), 6.55 (d, 1H, J= 15.99 Hz), 4.81-4.79 (m, 1H), 4.49 (s, 1H), 3.87 (s, 3H), 3.80 (s, 3H), 3.75 (s, 3H), 3.42 (s, 3H), 3.14-3.13 (m, 3H), 2.94-2.85 (m, 3H), 2.68-2.66 (m, 1H), 2.21-2.16 (m, 1H), 1.99-1.74 (m, 6H); ^{13}C NMR (125 MHz, DMSO, δ): 172.07, 168.17, 166.19, 159.75, 155.79, 144.34, 137.13, 132.76, 130.86, 126.43, 123.99, 121.87, 118.53, 116.70, 113.15, 108.81, 106.24, 95.28, 79.59, 77.91, 77.02, 60.64, 56.41, 55.67, 53.97, 52.31, 51.31, 50.96, 48.69, 33.17, 32.12, 29.67, 23.67, 16.57; ESI-MS: m/z= 619.3 (M^+ + H); Anal. Calcd for $C_{34}H_{38}N_2O_9.3H_2O$: C, 60.70; H, 6.59; N, 4.16; Found: C, 60.76; H, 6.39; N, 4.07.

For 5 (R_1 = OCH_3, R_2 = OH): White flakes from chloroform, yield = 108 mg (27%), (chloroform/methanol 4%, R_f = 0.3), mp = 259-260 ^{o}C; ^1H NMR (300 MHz, DMSO, δ): 10.49 (s, 1H), 9.61 (s, br, 1H), 7.62 (d, 1H, J=

15.87 Hz), 7.35 (s, 1H), 7.21 (d, 1H, J= 8.48 Hz), 7.14 (d, 1H, J= 8.35Hz), 6.82-6.79 (m, 2H), 6.61 (d, 1H, J= 8.49 Hz), 6.50 (d, 1H, J= 15.89 Hz), 4.87-4.78 (m, 1H), 4.33 (s, 1H), 3.83 (s, 3H), 3.78 (s, 3H), 3.75 (s, 3H), 3.41 (s, 3H), 3.04-3.01 (m, 2H), 2.87-2.81 (m, 2H), 2.66-2.63 (m, 1H), 2.36- 2.31 (m, 2H), 2.19-2.12 (m, 1H), 2.04- 2.00 (m, 1H), 1.93-1.69 (m, 5H); ^{13}C NMR (75 MHz, DMSO, δ): 172.88, 166.49, 156.23, 148.72, 145.98, 144.79, 136.34, 130.55, 128.02, 122.22, 121.86, 118.55, 116.23, 113.18, 110.59, 109.05, 108.13, 95.20, 77.84, 65.84, 60.77, 55.99, 55.82, 53.71, 51.78, 51.19, 49.06, 34.04, 32.34, 29.69, 24.28, 16.81, 15.26; ESI-MS: m/z= 591.2 (M^+ + H).

For 6 (R_1 = OH, R_2 = OCH_3): Yellow solid recrystallized from diethyl ether, yield = 174 mg (43%), (chloroform/methanol 3%, R_f = 0.3), mp = 180-182 ^{o}C; ^{1}H NMR (300 MHz, $CDCl_3$, δ): 7.77 (s, 1H), 7.63 (d, 1H, J= 15.92 Hz), 7.36 (d, 1H, J= 8.54 Hz), 7.32 (d, 1H, J= 8.54 Hz), 7.27 (s, 1H), 6.97 (d, 1H, J= 8.56 Hz), 6.82 (s, 1H), 6.76 (d, 1H, J= 8.53 Hz), 6.33 (d, 1H, J= 15.92 Hz), 4.95-4.87 (m, 1H), 4.42 (s, 1H), 3.85 (s, 3H), 3.82 (s, 3H), 3.81 (s, 3H), 3.50 (s, 3H), 3.49-3.44 (m, 2H), 3.18-3.14 (m, 2H), 3.02-2.97 (m, 1H), 2.67-2.62 (dd, 1H), 2.49-2.39 (m, 3H), 2.33 (s, 3H), 2.04-1.78 (m, 5H).; ^{13}C NMR (125 MHz, $CDCl_3$, δ): 172.86, 168.88, 166.34, 156.18, 152.97, 143.86, 140.06, 136.38, 130.57, 127.82, 127.50, 122.21, 121.94, 118.51, 116.76, 112.35, 108.98, 107.99, 95.25, 77.87, 65.84, 60.79, 56.02, 55.82, 53.74, 51.79, 51.23, 49.04, 34.03, 32.32, 29.69, 24.25, 20.62, 16.81, 15.27; ESI-MS: m/z= 6.33.3 (M^+ + H); Anal. Calcd for $C_{35}H_{40}N_2O_9.0.25H_2O$: C, 65.97; H, 6.41; N, 4.40; Found: C, 65.74; H, 6.55; N, 4.49.

For 7 (R_1 = $OCOCH_3$, R_2 = OCH_3): Yellow solid recrystallized from diethyl ether, yield = 174 mg (43%), (chloroform/methanol 3%, R_f = 0.3), mp = 180-182 ^{o}C; ^{1}H NMR (300 MHz, $CDCl_3$, δ): 7.77 (s, 1H), 7.63 (d, 1H, J= 15.92 Hz), 7.36 (d, 1H, J= 8.54 Hz), 7.32 (d, 1H, J= 8.54 Hz), 7.27 (s, 1H), 6.97 (d, 1H, J= 8.56 Hz), 6.82 (s, 1H), 6.76 (d, 1H, J= 8.53 Hz), 6.33 (d, 1H, J= 15.92 Hz), 4.95-4.87 (m, 1H), 4.42 (s, 1H), 3.85 (s, 3H), 3.82 (s, 3H), 3.81 (s, 3H), 3.50 (s, 3H), 3.49-3.44 (m, 2H), 3.18-3.14 (m, 2H), 3.02-2.97 (m, 1H), 2.67-2.62 (dd, 1H), 2.49-2.39 (m, 3H), 2.33 (s, 3H), 2.04-1.78 (m, 5H).; ^{13}C NMR (125 MHz, $CDCl_3$, δ): 172.86, 168.88, 166.34, 156.18, 152.97, 143.86, 140.06, 136.38, 130.57, 127.82, 127.50, 122.21, 121.94, 118.51, 116.76, 112.35, 108.98, 107.99, 95.25, 77.87, 65.84, 60.79, 56.02, 55.82, 53.74, 51.79, 51.23, 49.04, 34.03, 32.32, 29.69, 24.25, 20.62, 16.81, 15.27; ESI-MS: m/z= 6.33.3 (M^+ + H); Anal. Calcd for $C_{35}H_{40}N_2O_9.0.25H_2O$: C, 65.97; H, 6.41; N, 4.40; Found: C, 65.74; H, 6.55; N, 4.49.

Propionoyl reserpate (8). Using the same procedure for 1 and substituting propionyl chloride for acryloyl chloride yields a residue that was purified by flash chromatography (silica gel, chloroform/methanol, 3%, R_f 0.2) to give a solid that was rinsed with methanol/diethylether (1:1) to afford 8 (317 mg, 56%) as a fine light yellow powder : mp = 258 ^{o}C; ^{1}H-NMR (300 MHz, $CDCl_3$, δ): 7.60 (br, s, 1H), 7.32 (d, 1H, J= 8.54 Hz), 6.82 (s, 1H), 6.76 (d, 1H, J= 8.59 Hz), 4.81-4.72 (m, 1H), 4.41 (s, 1H), 3.83 (s, 3H), 3.80 (s, 3H), 3.74-3.71 (m, 1H), 3.49 (s, 3H), 3.24-3.10 (m, 2H), 3.03-2.88 (m, 2H), 2.63-2.58 (m, 1H), 2.50-2.31 (m, 2 H), 2.28-2.12 (m, 4H), 2.03-1.75 (m, 4H), 1.17 (t, 3H, J= 1.35, 7.39 Hz); ^{13}C-NMR (75 MHz, $CDCl_3$, δ): 173.79, 172.52, 156.21, 136.42, 130.53, 122.27, 118.52, 109.02, 108.05, 95.34, 77.74, 77.32, 60.61, 55.83, 53.73, 51.78, 51.69, 51.22, 49.05, 34.01, 32.33, 29.55, 28.03, 24.25, 16.80, 9.16.; ESI-MS: m/z= 471.3 (M^+ + H); Anal. Calcd. for $C_{26}H_{34}N_2O_6$C, 66.36; H, 7.28; N, 5.95. Found: C, 66.08; H, 7.44; N, 5.87.

5-iodo-2-methoxyphenyl acetate (9). 2-Methoxyphenylacetate (28.5 g, 171.87 mmol) was added to a mixture of iodine (17.46 g, 68.75 mmol) and HIO_3 (7.18 g, 40.8 mmol) in glacial acetic acid (190 mL), chloroform (50 mL), water (65 mL) and concentrated sulfuric acid (2 mL) and this mixture was stirred for 24 h at 40^{o}C. Chloroform (50 mL) and water (30mL) were added and the mixture was washed with dilute $NaHSO_3$ (3X) and water. The organic layer was dried with magnesium sulfate and the organic solvent was removed under vacuum to leave a residue that was recrystallized from ethanol to afford 9 as white crystals (11.7 g, 23%); (chloroform/methanol 2%, R_f, 0.3), m.p = 75 °C; ^{1}H-NMR (300 MHz, $CDCl_3$, δ): 7.49-7.46 (dd, 1H J= 8.63, 2.15 Hz), 7.34 (d, 1H, J= 2.17 Hz), 6.73 (d, 1H, J= 8.66 Hz), 3.79 (s, 3H), 2.29 (s, 3H); ^{13}C-NMR (75 MHz, $CDCl_3$, δ): 168.58, 151.37, 140.48, 135.71, 131.62, 114.33, 81.32, 55.98, 20.55; ESI-MS: m/z= 292.9 (M^+); Anal. Calcd. for $C_9H_9IO_3.0.5CH_3COOH$ C, 37.29; H, 3.44. Found: C, 37.92; H, 3.09.

N-hydroxy-5-iodo-2-methoxybenzamide (10). Separate solutions of hydroxylamine hydrochloride (605 mg, 8.60 mmole) in methyl alcohol (75 mL) and potassium hydroxide (1.2 g, 18.81 mmole) in methanol (50 mL) are prepared at the boiling point of the solvent. Both are cooled to 30-40 °C and the one containing alkali was added with shaking to the solution of hydroxylamine; any excessive rise of temperature during the addition is prevented by occasional cooling in an ice bath. After all the alkali has

been added, the mixture is allowed to stand in an ice bath for 5 min to ensure complete precipitation of potassium chloride followed by filtration. The filtrate was added to methyl 5-iodo-2-methoxybenzoate (500 mg, 1.72 mmole) and the mixture was heated to reflux for 6 h and cooled to room temperature. The mixture was acidified with glacial acetic acid until the pH was about 6 and concentrated to remove the solvents. The residue was mixed with EtOAc (100 mL) and water (80 mL) was added to get a clear solution. The organic layer was separated and the aqueous solution was extracted with EtOAc (2 x 50 mL). The combined organic phases were washed with brine, dried over anhydrous sodium sulfate, and concentrated to afford a white solid residue, recrystallized from chloroform to afford 9 as white crystals (362 mg, 73% yield) (ethyl acetate/ hexane 1:5, R_f=0.3); mp = 157-158°C; ^{1}H-NMR (300 MHz, DMSO, δ): 10.68 (s, 1H), 9.16 (br, s, 1H), 7.82-7.72 (m, 2H), 7.01-6.93 (d, 1H, J = 8.62 Hz), 3.81 (s, 3H); ^{13}C-NMR (75 MHz, DMSO, δ): 161.50, 156.48, 139.93, 137.55, 124.89, 114.64, 82.73, 55.85; ESI-MS: m/z= 294.0 (M^+ + 1); Anal. Calcd. for $C_8H_8INO_3$ C, 32.79; H, 2.75; N, 4.78. Found: C, 32.82; H, 2.61; N, 4.79.

N-hydroxy-4-iodo-2-methoxybenzamide (11). This compound was prepared using the same procedure for 7 with methyl-4-iodo-2-methoxybenzoate as substrate to afford an off-white solid that was recrystallized from ethyl acetate/n-hexane to yield 10 as off-white crystals (102 mg, 21%); (ethyl acetate/ hexane 1:5, R_f=0.4); mp = 105-106°C; ^{1}H-NMR (300 MHz, $CDCl_3$, δ): 10.24 (s, br, 1H), 7.82 (d, 1H, J = 8.23 Hz), 7.41 (d, 1H, J = 8.12 Hz), 7.28 (s, 1H), 3.95 (s, 3H); ^{13}C-NMR (75 MHz, $CDCl_3$, δ): 163.13, 157.03, 132.89, 130.94, 120.77, 118.01, 99.66, 56.52; ESI-MS: m/z= 294.0 (M^+ + 1); Anal. Calcd. for $C_8H_8INO_3.0.1CH_3COOC_2H_5$ C, 33.42; H, 2.94; N, 4.64. Found: C, 33.48; H, 2.76; N, 4.57.

General procedure for synthesis of rescinnamine derivatives (12-15): A similar Heck coupling procedure without a phosphine ligand using the appropriate substituted aryl iodides affords the corresponding substituted rescinnamine derivatives (12-15).

For 12: Yellowish brown solid recrystallized from diethyl ether, yield = 132 mg (35%), (chloroform/methanol 2%, R_f= 0.2), mp = 202-203 ^{o}C; ^{1}H NMR (300 MHz, $CDCl_3$, δ): 7.66 (s, 1H), 7.63 (d, J = 15.91 Hz, 1H), 7.32 (d, J = 8.54 Hz, 1H), 6.94-6.90 (m, 2H), 6.82 (s, 1H), 6.74 (d, J = 8.70 Hz, 2H), 6.27 (d, J = 15.88 Hz, 1H), 4.96-4.87 (m, 1H), 4.44 (s, 1H), 3.88 (s, 3H), 3.83 (s, 3H), 3.81 (s, 3H), 3.51 (s, 3H), 3.42-3.44 (m, 1H), 3.20-3.15 (m, 2H), 3.04-2.89 (m, 2H), 2.73-2.61(m, 1H), 2.50-2.42 (m, 2H), 2.29-2.17 (m, 2H), 2.05-1.77 (m, 4H), 1.28-1.18 (m, 2H); ^{13}C NMR (75 MHz, $CDCl_3$, δ): 172.92, 166.68, 156.23, 149.42, 145.33, 136.54, 136.38, 130.51, 127.47, 122.21, 120.30, 118.53, 115.41, 113.13, 110.18, 109.05, 108.06, 95.23, 77.88, 65.84, 60.75, 55.83, 55.59, 53.75, 51.78, 51.21, 49.08, 34.04, 32.32, 29.74, 24.27, 16.81, 15.26; ESI-MS: m/z= 590 (M^+ + 1), 295 (M^+ + 2). HRMS-ESI$^+$ (m/z): [M + H]$^+$ calcd for $C_{33}H_{40}N_3O_7$, 590.2866; found, 590.2846; Anal. Calcd for $C_{33}H_{39}N_3O_7.0.8H_2O$: C, 65.61; H, 6.77; N, 6.96; Found: C, 65.27; H, 6.63; N, 6.87.

For 13: Pale yellow flakes recrystallized from diethyl ether, yield = 153 mg (41%), (chloroform/methanol 2%, R_f= 0.4), mp = 210-213 ^{o}C; ^{1}H NMR (300 MHz, $CDCl_3$, δ): 7.81 (s, br, 1H), 7.61 (d, J = 15.8.4 Hz, 1H), 7.31 (d, J = 8.54 Hz, 1H), 7.01 (d, J = 7.98 Hz, 1H), 6.96 (s, 1H), 6.82 (s, 1H), 6.75 (d, J = 8.54 Hz, 1H), 6.66 (d, J = 7.97 Hz, 1H), 6.23 (d, J = 15.83 Hz, 1H), 4.95-4.80 (m, 1H), 4.43 (s, br, 1H), 4.14 (s, 1H), 3.88 (s, 3H), 3.82 (s, 3H), 3.80 (s, 3H), 3.50 (s, 3H), 3.18-3.13 (m, 2H), 3.03-2.93 (m, 2H), 2.67-2.58 (m, 1H), 2.49-2.40 (m, 2H), 2.27-2.16 (m, 2H), 1.92-1.77 (m, 5H); ^{13}C NMR (75 MHz, $CDCl_3$, δ): 172.99, 166.94, 156.15, 146.97, 145.77, 139.20, 136.36, 130.51, 128.67, 124.60, 123.34, 122.15, 118.52, 114.06, 113.39, 108.98, 107.96, 95.19, 60.77, 55.82, 55.50, 53.73, 51.82, 51.19, 49.03, 41.81, 34.01, 32.30, 30.95, 29.77, 24.24, 16.78, 13.85; ESI-MS: m/z= 590 (M^+ + 1), Anal. Calcd for $C_{33}H_{39}N_3O_7.0.6H_2O$: C, 66.01; H, 6.75; N, 7.00; Found: C, 66.11; H, 6.64; N, 6.71.

For 14: Grayish white solid, yield = 289 mg (70%), recrystallized from benzene, (chloroform/methanol 6%, R_f= 0.3), mp = 245-255 ^{o}C; ^{1}H NMR (500 MHz, DMSO, δ): 10.96 (s, 1H), 7.57 (s, 1H), 7.49 (d, 1H, J= 15.78 Hz), 7.37-7.34 (m, 2H), 7.23 (s, 1H), 6.86 (s, 1H), 6.71 (d, 1H, J= 8.49 Hz), 6.27 (d, 1H, J= 15.79 Hz), 5.06 (s, br, 1H), 5.06 (s, 1H), 4.69-4.72 (m, 1H), 3.81 (s, 3H), 3.79 (s, 3H), 3.77 (s, 3H), 3.74-3.68 (m, 2H), 3.65-3.57 (m, 1H), 3.44 (s, 3H), 3.17-3.07 (m, 1H), 2.84-2.99 (m, 1H), 2.85-2.82 (m, 1H), 2.73-2.69 (m, 1H), 2.30-2.08 (m, 5H), 1.94-1.83 (m, 2H); ^{13}C NMR (125 MHz, DMSO, δ): 171.76, 171.24, 165.79, 157.77, 155.92, 149.02, 147.59, 145.74, 137.31, 128.29, 124.66, 122.56, 120.84, 120.64, 118.63, 118.35, 112.76, 112.08, 109.04, 105.34, 94.82, 77.12, 75.66, 60.23, 55.66, 55.25, 54.32, 51.95, 50.16, 31.27, 30.34, 28.34,

22.49, 15.49; ESI-MS: m/z= 635.2 (M^+ + H); HRMS: [M^+ + H- CH_3] calcd for $C_{34}H_{39}N_2O_{10}$, 635.2605; found, 635.2582; Anal. Calcd for $C_{35}H_{40}N_2O_{10}.2.5H_2O$: C, 61.71; H, 6.25; N, 4.23; Found: C, 61.84; H, 5.87; N, 4.28. For 15: Dark yellow solid, yield = 140 mg (35%), recrystallized from diethyl ether, (chloroform/methanol 5%, R_f = 0.1), mp = 229-231 °C; ^{1}H NMR (300 MHz, DMSO, δ): 10.49 (s, 1H), 8.96 (s, br, 1H), 7.63 (d, 1H, J= 15.81 Hz), 7.20 (d, 1H, J= 8.57 Hz), 7.06 (s, 2H), 6.80 (s, 1H), 6.62-6.54 (m, 2H), 4.89-4.76 (m, 1H), 4.35 (s, 1H), 3.82 (s, 6H), 3.79 (s, 3H), 3.75 (s, 3H), 3.42 (s, 3H), 3.10-2.97 (m, 3H), 2.89-2.79 (m, 3H), 2.69-2.60 (m, 3H), 2.42-2.14 (m, 5H); ^{13}C NMR (75 MHz, DMSO, δ): 171.61, 165.98, 155.05, 148.01, 145.61, 138.35, 136.35, 131.20, 128.52, 124.37, 121.65, 117.81, 114.96, 108.01, 106.32, 105.92, 94.77, 77.54, 76.40, 64.87, 60.05, 56.09, 55.18, 53.32, 51.74, 51.05, 50.74, 48.62, 33.19, 32.14, 29.53, 23.46, 16.44, 15.12; ESI-MS: m/z= 621.3 (M^+ + H).

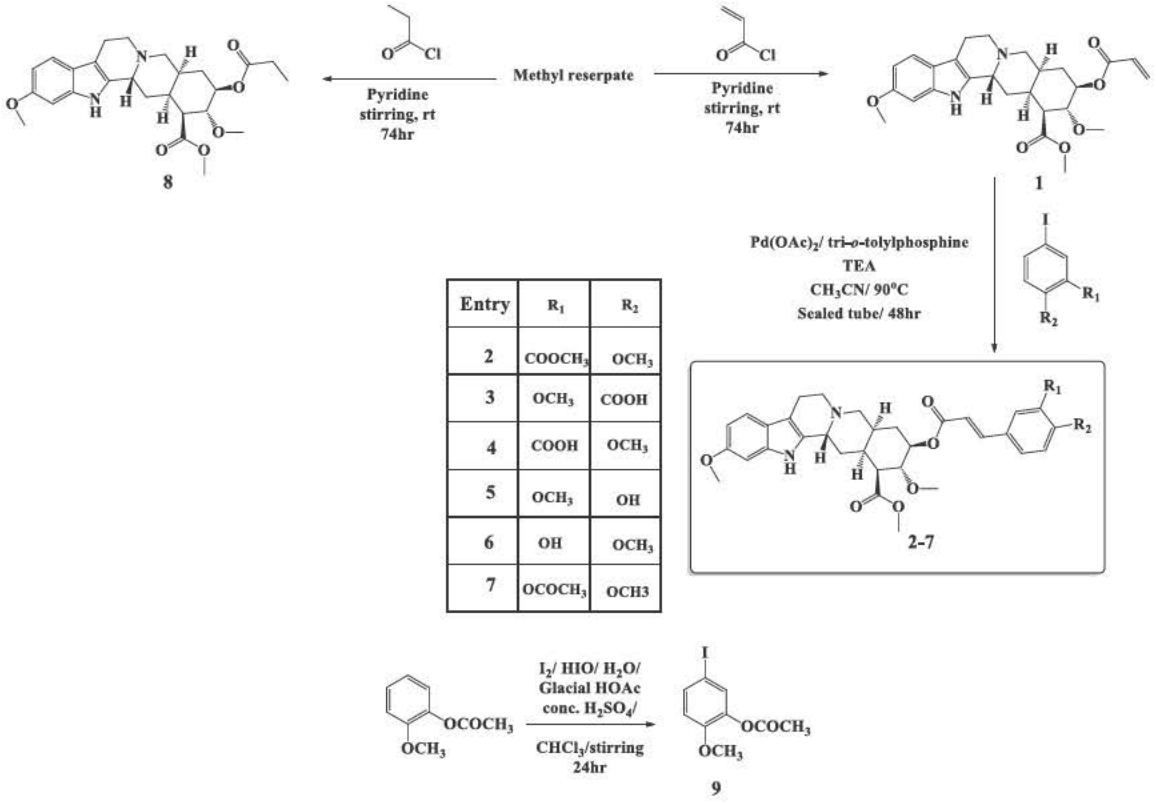

Entry	R_1	R_2
2	$COOCH_3$	OCH_3
3	OCH_3	COOH
4	COOH	OCH_3
5	OCH_3	OH
6	OH	OCH_3
7	$OCOCH_3$	OCH3

Fig.5. Synthetic procedures for the preparation of rescinnamine derivatives (1-8). Condensation reactions between methyl reserpate and acyl chlorides to give 1 and 8. Heck coupling procedure with 1 to yield rescinnamine derivatives 2-7.

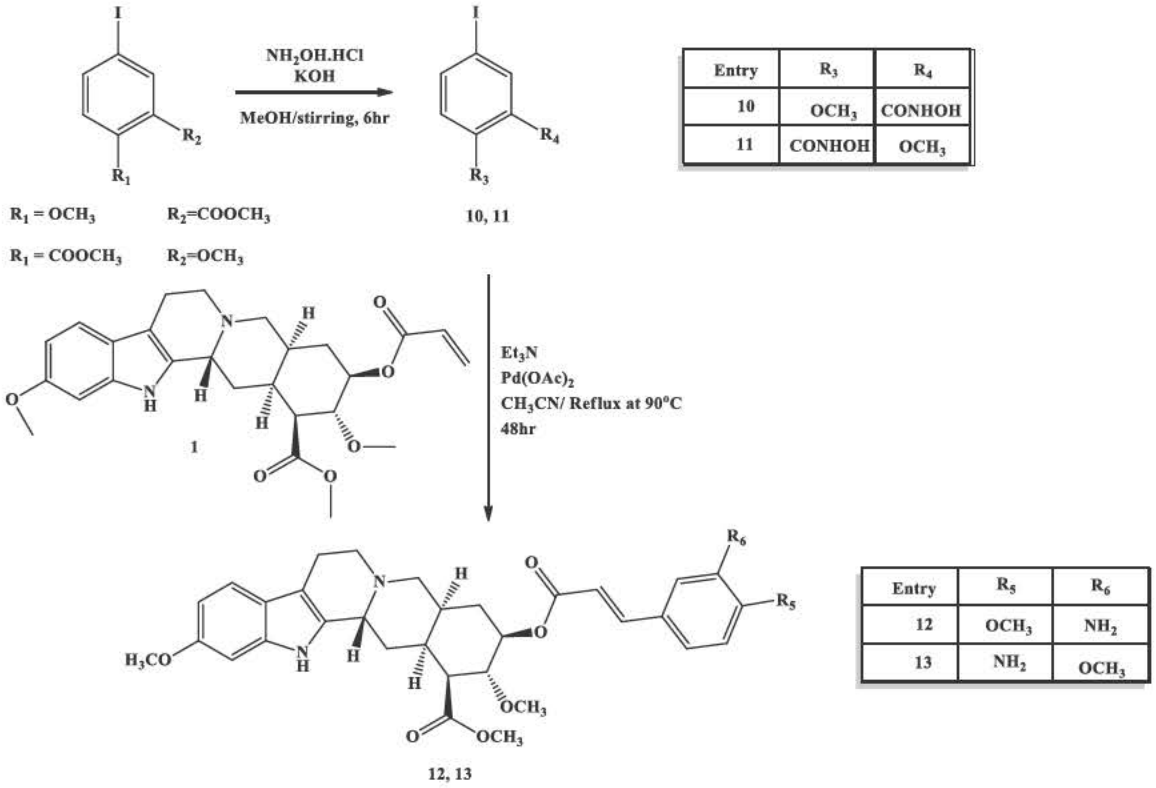

Entry	R_3	R_4
10	OCH_3	CONHOH
11	CONHOH	OCH_3

Entry	R_5	R_6
12	OCH_3	NH_2
13	NH_2	OCH_3

Fig.6. Synthetic procedures for the preparation of rescinnamine derivatives (12-13). Heck coupling of synthetic hydroxamic acid aryl iodides gives the amino-substituted rescinnamine derivatives 12 and 13.

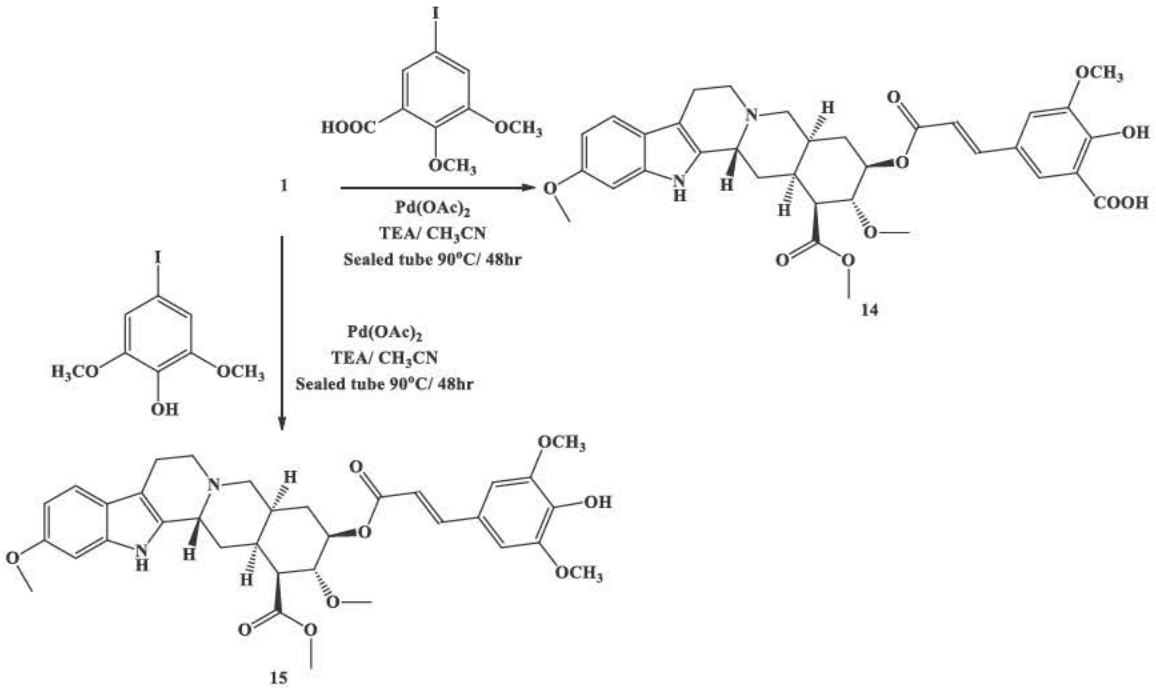

Fig. 7 (previous page). Synthetic procedures for the preparation of rescinnamine derivatives (14-15). Heck coupling of commercially available aryl iodides to give rescinnamine derivatives 14 and 15.

Prostate cancer cell lines were tested against these compounds as indicated in the SOW. We added HEC59, an endometrial cell line with an MSH2 deficiency and its counterpart HEC59 chr.2 with complemented MSH2 to some of the tests to determine if the new compounds show the rescinnamine-specific specificity for MSH2.
Promising lead molecules that were predicted to induce MSH2-dependent cell death and had a favorable partition coefficient were considered for chemical synthesis (Table 1).
Treatment of methyl reserpate, formed by the basic methanolysis of reserpine (Vasilyeva et al., 2010), with acryloyl chloride yields acryloyl reserpate (1) in 35% yield (Figure 5) (Pearce et al., 1989). Similar treatment of 1 with propionoyl chloride yields the saturated derivative 8. Exposure of 1 to various commercial or synthetic substituted aryl iodides (9) to palladium catalyzed Heck coupling conditions gives the di-substituted rescinnamine derivatives (2-7) in 27-68% yield and coupling constant analysis shows the exclusive formation of the trans stereoisomer (Figure 5) (Ziegler et al., 1978). Condensation of the commercially available methyl esters with hydroxylamine produces the corresponding hydroxamic acids (10 and 11, Figure 6) (Hoshino et al., 2009) and Heck coupling of 1 to 10 and 11 in the absence of a phosphine ligand yields the aniline derivatives of rescinnamine (9 and 10, exclusive E stereochemistry) in 35 and 41% yield, respectively rather than the expected hydroxamic acids (Figure 6). (Patel et al., 1977) Such results suggest either a base or palladium-mediated Lossen rearrangement of these hydroxamic acid substrates, a process that holds some literature precedence (Hoshino et al., 2009). Similar Heck coupling of 1 to commercial aryl iodides yields the tri-substituted rescinnamine derivatives 14 and 15 in 70 and 35% yield, respectively (Figure 7). Extensive mass spectrometry and two-dimensional nuclear magnetic resonance (NMR) experiments confirm the structure of 14, which lacks the expected p-methoxy group of the starting material (Figure 7). A combination of proton and carbon NMR spectroscopy, mass spectrometry and elemental analysis confirms the identity of 1-15.

Effects of rescinnamine analogs on cell viability:
We next tested these new rescinnamine analogs in a well-defined cellular system with an endometrial cell line deficient (HEC59) and proficient (via chromosome transfer, HEC59 + chr.2) for MSH2. This cell system allows to determine whether our new analogs hit their target and, generally, induce cell death. The assays identified a few compounds that induced cell killing in the micromolar range (Figure 8 and Table 1). However, little significant MSH2-dependence was observed for most of these compounds. No significant difference was detected when determining the IC50 values and these results are surprising in-light of our previous work. Previous studies have suggested that in addition to MSH2-dependent cell-killing due to rescinnamine and derivatives, there is off-target cell-killing as well (Vasilyeva et al., 2010). These results suggest considerable off-target killing for these classes of compounds.
Compounds 84-90 do not show significant specificity for MSH2, either, but compound 81 shows significant cell death with minor specificity for MSH2.

A

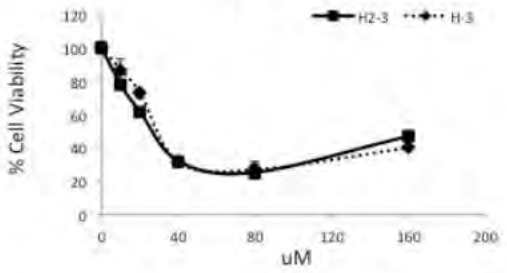
SA-I-03
H2-3
H-3
% Cell Viability
uM

B

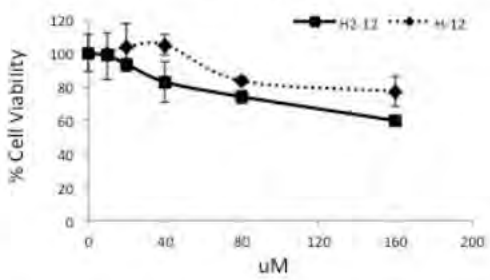
SA-I-12
H2-12
H-12
% Cell Viability
uM

C

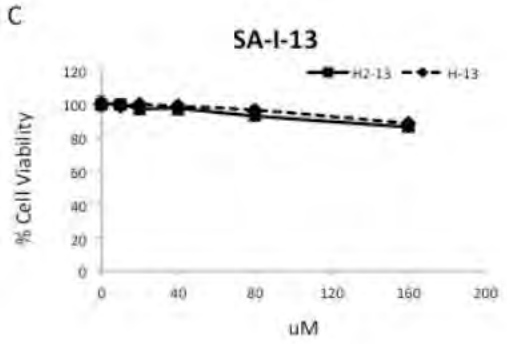
SA-I-13
H2-13
H-13
% Cell Viability
uM

D

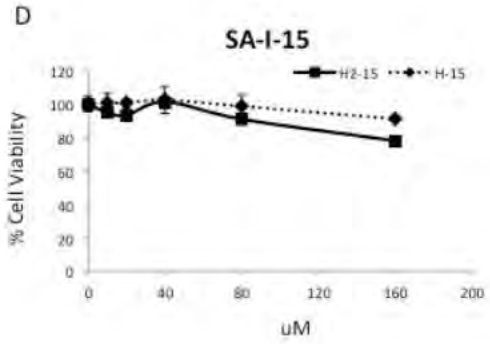
SA-I-15
H2-15
H-15
% Cell Viability
uM

E

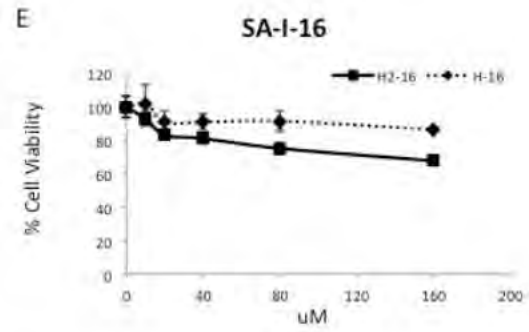
SA-I-16
H2-16
H-16
% Cell Viability
uM

F

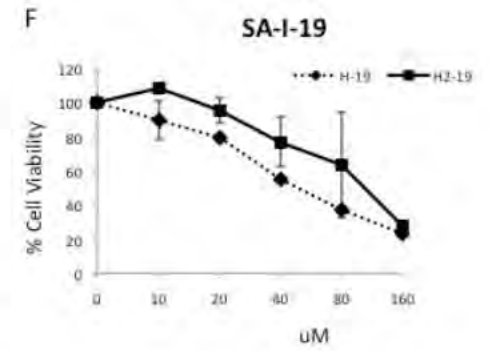
SA-I-19
H-19
H2-19
% Cell Viability
uM

G

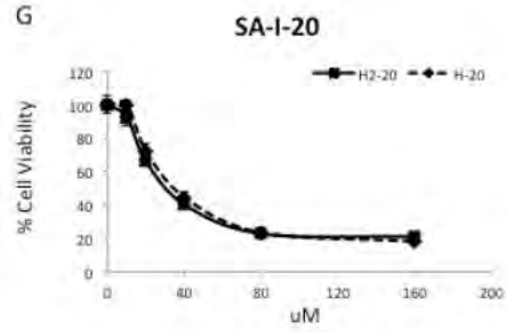
SA-I-20
H2-20
H-20
% Cell Viability
uM

H

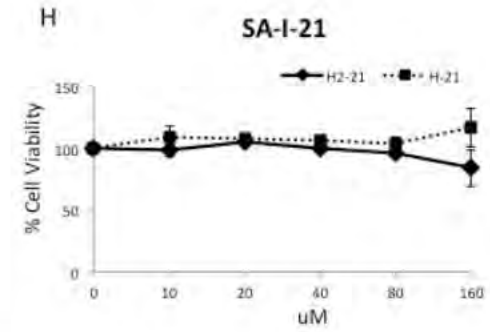
SA-I-21
H2-21
H-21
% Cell Viability
uM

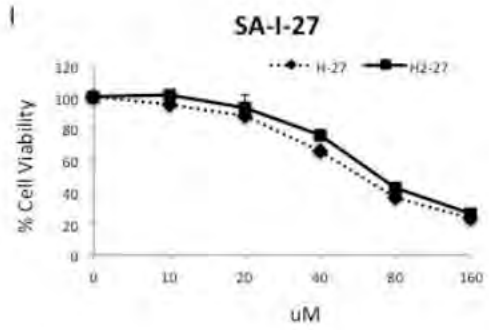
I
SA-I-27
H-27
H2-27
% Cell Viability
uM

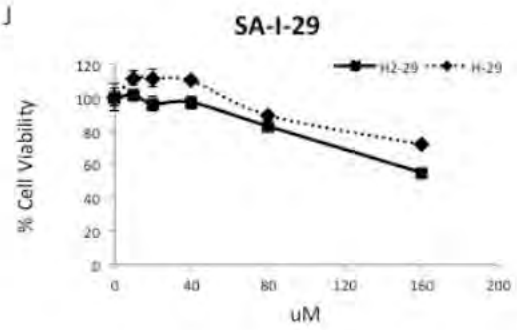
J
SA-I-29
H2-29
H-29
% Cell Viability
uM

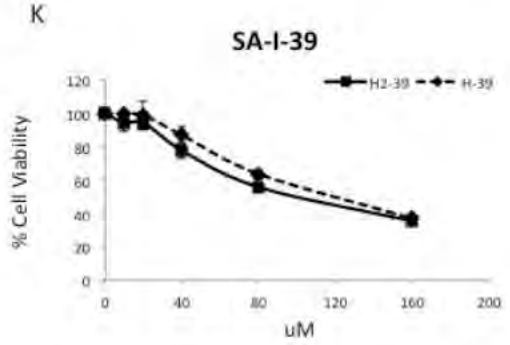
K
SA-I-39
H2-39
H-39
% Cell Viability
uM

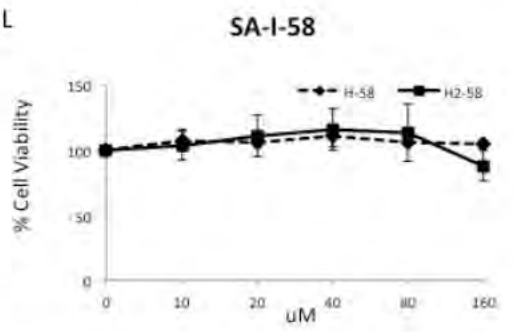
L
SA-I-58
H-58
H2-58
% Cell Viability
uM

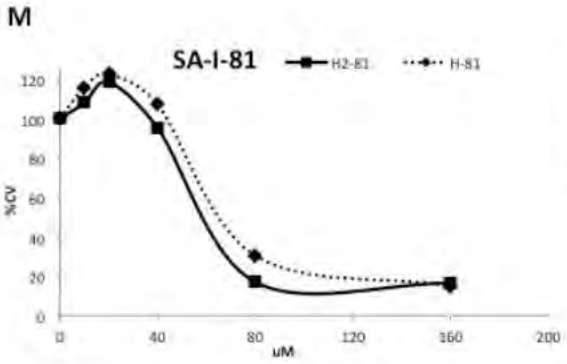
M
SA-I-81
H2-81
H-81
%CV
uM

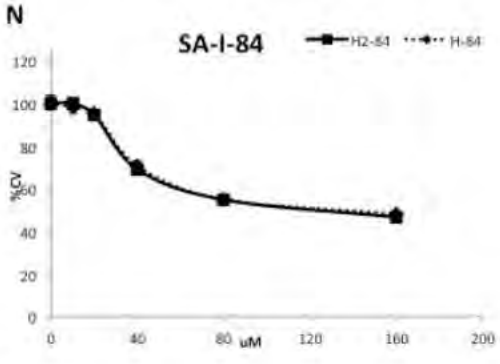
N
SA-I-84
H2-84
H-84
%CV
uM

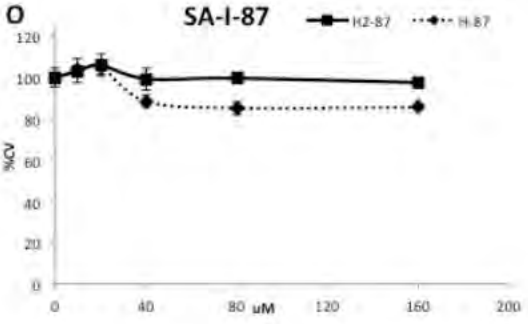
O
SA-I-87
H2-87
H-87
%CV
uM

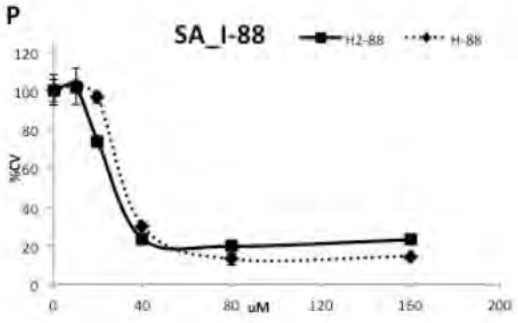
P
SA_I-88
H2-88
H-88
%CV
uM

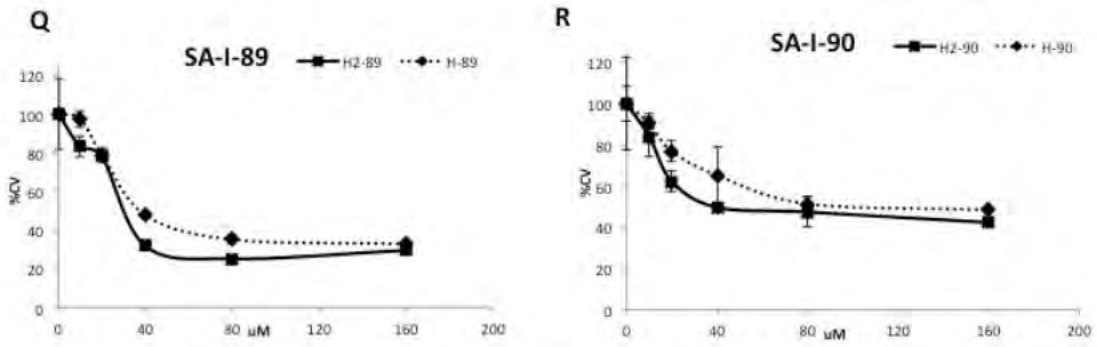

Fig. 8. ***Cell Survival of MSH2 proficient and deficient cells after treatment with rescinnamine analogs. HEC59 ("H") and its isogenic cell line containing a chromosome 2 transfer ("H2") were treated with increasing concentrations of the indicated compound (Table 1). Cell viability is graphed in dependence of concentration. CV: Cell Viability.***

Table 1: IC50 values for individual rescinnamine analogs. Where appropriate, graphs that did not reach 50& mortality were extrapolated. NA: no extrapolation possible.

		IC50	
Entry	**Compound**	MSH2 deficient	MSH2 proficient
SA-I-03	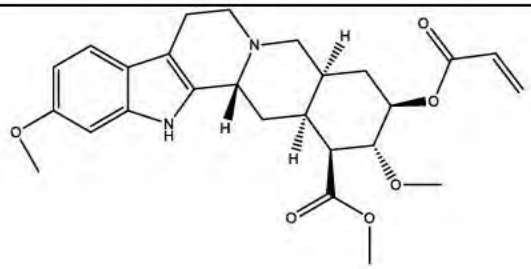	20.7	20.37
SA-I-058	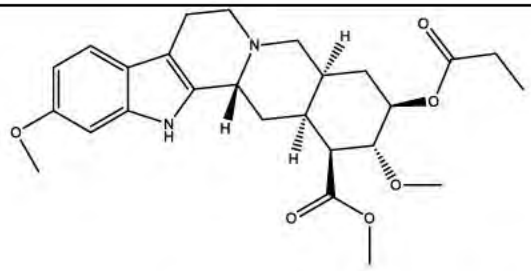	NA	NA
SA-I-012	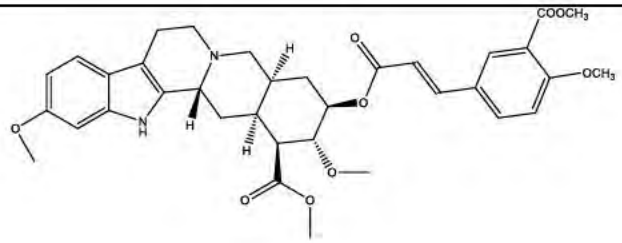	50.72	48.91

SA-I-013	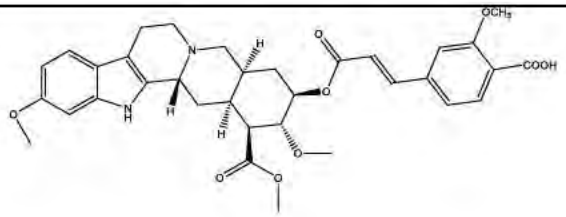	163.1	1223
SA-I-015	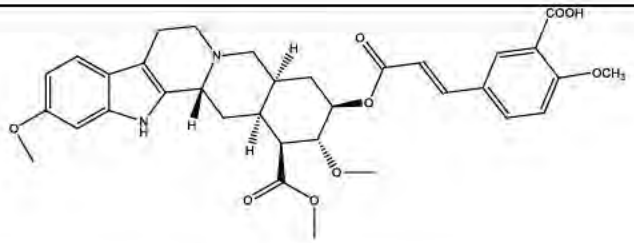	89.29	84.23
SA-I-016	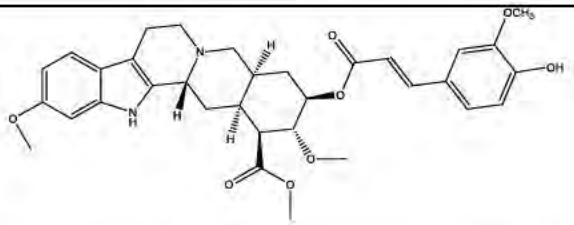	NA	NA
SA-I-020	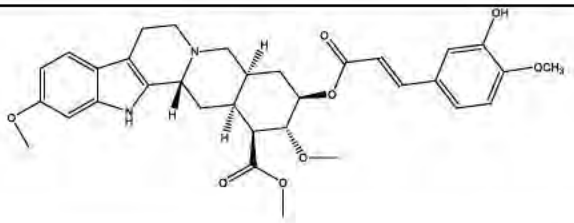	22.32	21.29
SA-I-019	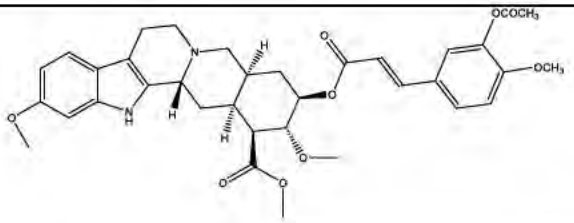	39.28	NA
SA-I-021	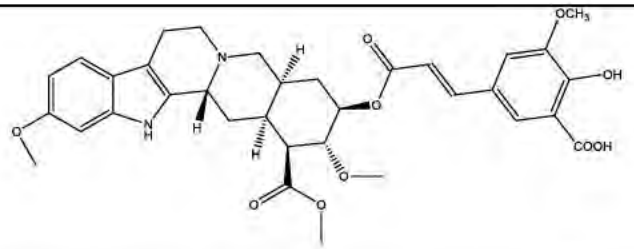	NA	NA
SA-I-027	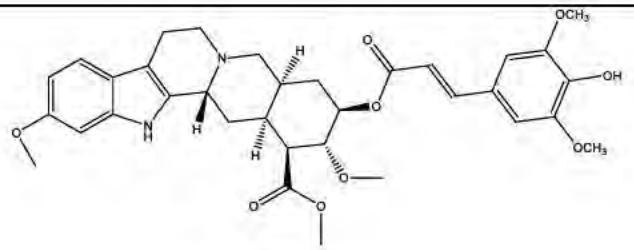	47.67	54.53

SA-I-029	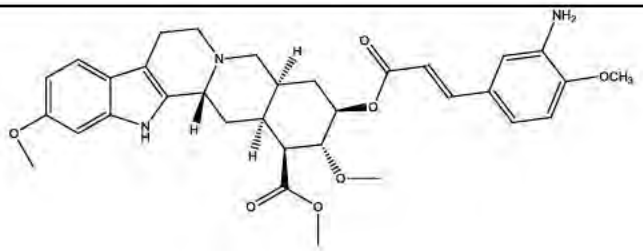	77.25	113.4
SA-I-039	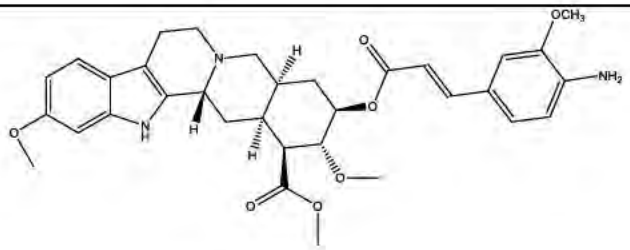	85.73	68.38
SA-I-81	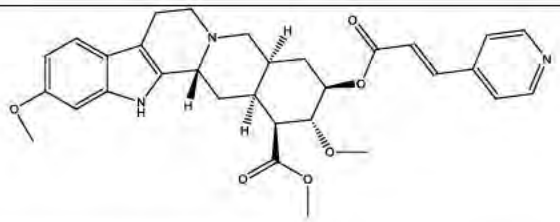	58.23	47.63
SA-I-84	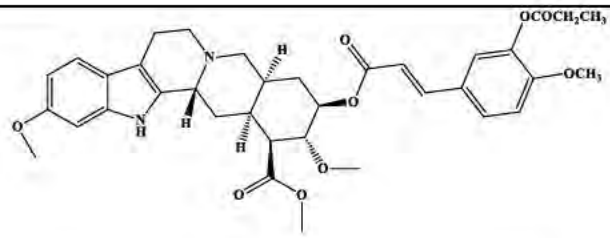	37.3	35.6
SA-I-87	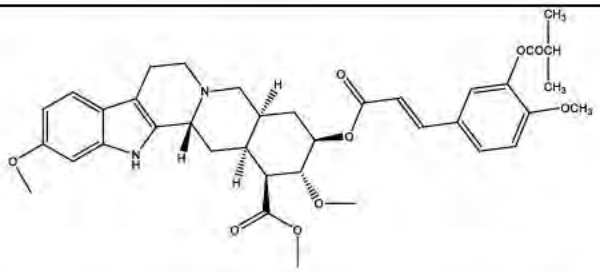	NA	NA
SA-I-88	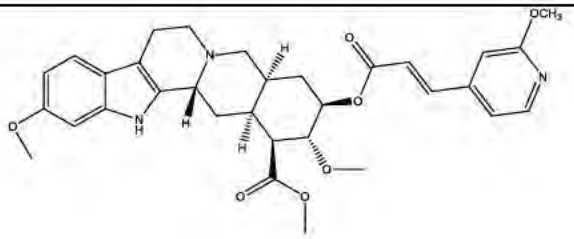	31.3	22.0
SA-I-89	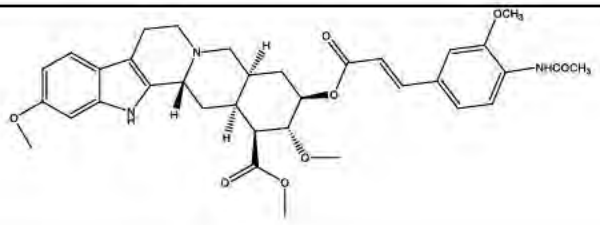	25.6	27.8

SA-I-90	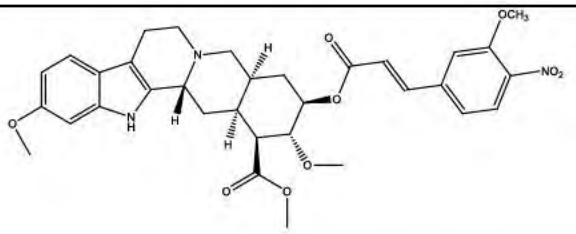	24.1	4.8

We repeated the cell viability assay for the most promising compounds, 12, 19 and 81 and performed a caspase-3 activation assay to determine induction of apoptosis (Figure 9).

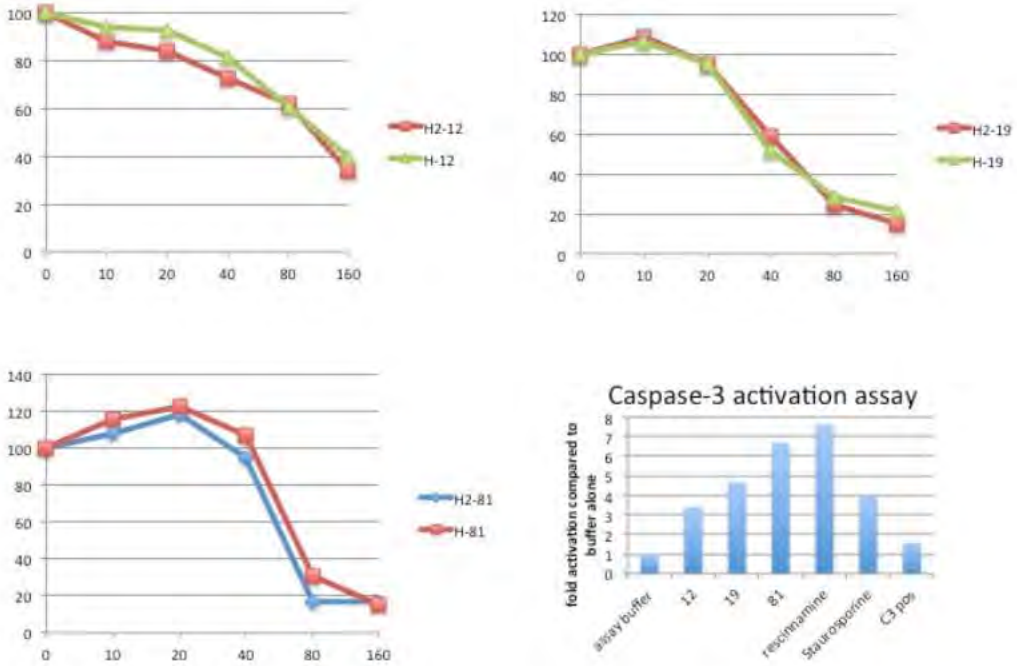

Fig. 9. Dose-dependent MTS assay with compounds 12, 19 and 81 in HEC59/HEC59chr.2 cells. Caspase-3 activation kit shows activation of the caspase as a measure of apoptosis. The assay was performed as recommended by the manufacturer. C3 pos is the included positive control. Staurosporine and rescinnamine are added as additional positive controls. All data are fold increase in comparison to "assay buffer", which was defined as "1". CV: Cell Viability

While no significant specificity for MSH2 is observed, compounds 19, 81 and 88 show significant cell killing ability that is dose-dependent. Both compounds activate caspase -3, similar to rescinnamine.

We next tested the most promising compounds against prostate cancer cells, and used A2780 cells (ovarian cancer) as a control, as before.

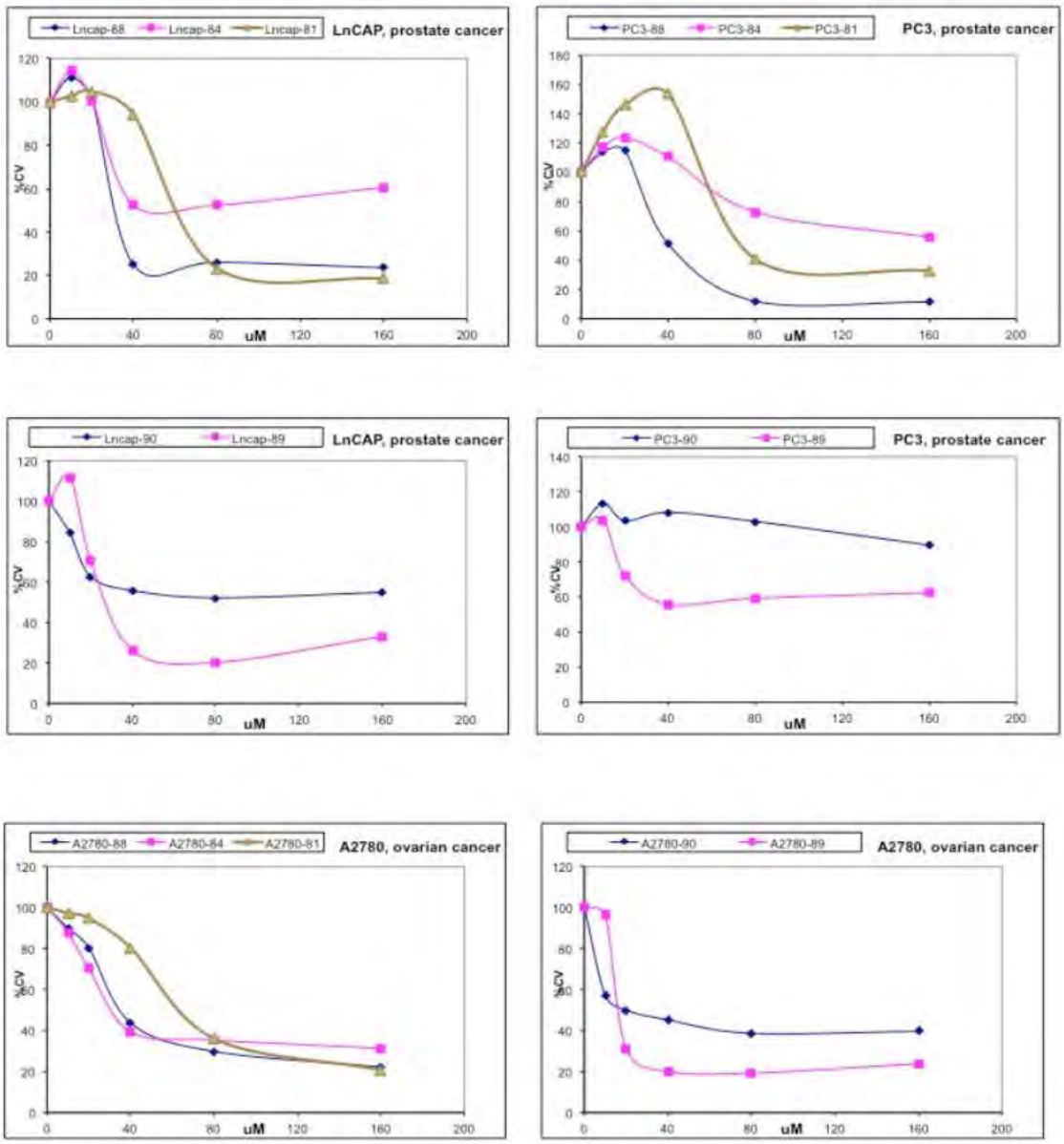

Fig. 10. Dose-dependent MTS assay with compounds 81, 84 and 88 in prostate cancer cells. *CV: Cell viability. Ovarian cancer cell line A2780 added as control.*

As was already observed in HEC59 cells, a threshold around 25 uM appears to exist beyond which cell viability is drastically reduced. For compound 81, the concentration at which this significant reduction in cell viability occurs, appears to be shifted to slightly higher concentrations, around 40 uM. Compounds 84, 89 and 90 show the worst effect on cell viability in prostate cancer cells, though they have efficacy in the ovarian cancer cell line. Even in LnCAP cells, 89 and 90 show some efficacy, which is almost entirely gone in PC3 cells. Overall, in prostate cancer cells, compound SA-I-88 exhibits the best activity, followed by SA-I-81 at this point (Table 2).

Table 2: IC50 values for individual rescinnamine analogs in prostate cancer cells. Where appropriate, graphs that did not reach 50& mortality were extrapolated (in parentheses). NA: no extrapolation possible.

	LnCAP	**PC3**	**A2780**
SA-I-81	53.8	73.4	56.8
SA-I-84	(21.5)	(63.0)	23.6
SA-I-88	22.96	38.6	31.3
SA-I-89	20.1	(18.4)	16.5
SA-I-90	(36.6)	NA	36.9

Our next step would be the determination of effects on other prostate cancer cells to determine specificity for cancer. We will also determine caspase activation to demonstrate the induction of apoptosis.
It may further be required to use these data in advanced computational docking experiments and identify additional analogs that may show even better efficacy against prostate cancer.

Task 1c. Determine efficacy of new compounds in combination therapy
We next tested some of the most promising compounds in combination therapy with cisplatin.

Figure 11 demonstrates that Compound #12 does not improve treatment with cisplatin, and combination treatment is equally effective. Combination treatment with fixed concentrations of #12 with varying concentrations of cisplatin increases efficacy in taxol-resistant cells to some extent, while the opposite treatment is not effective, suggesting a specific mechanistic exclusion. MSH2 deficient cells (LnCAP) are equally sensitive to single or combination treatments, with is in difference to MSH2 proficient cells.

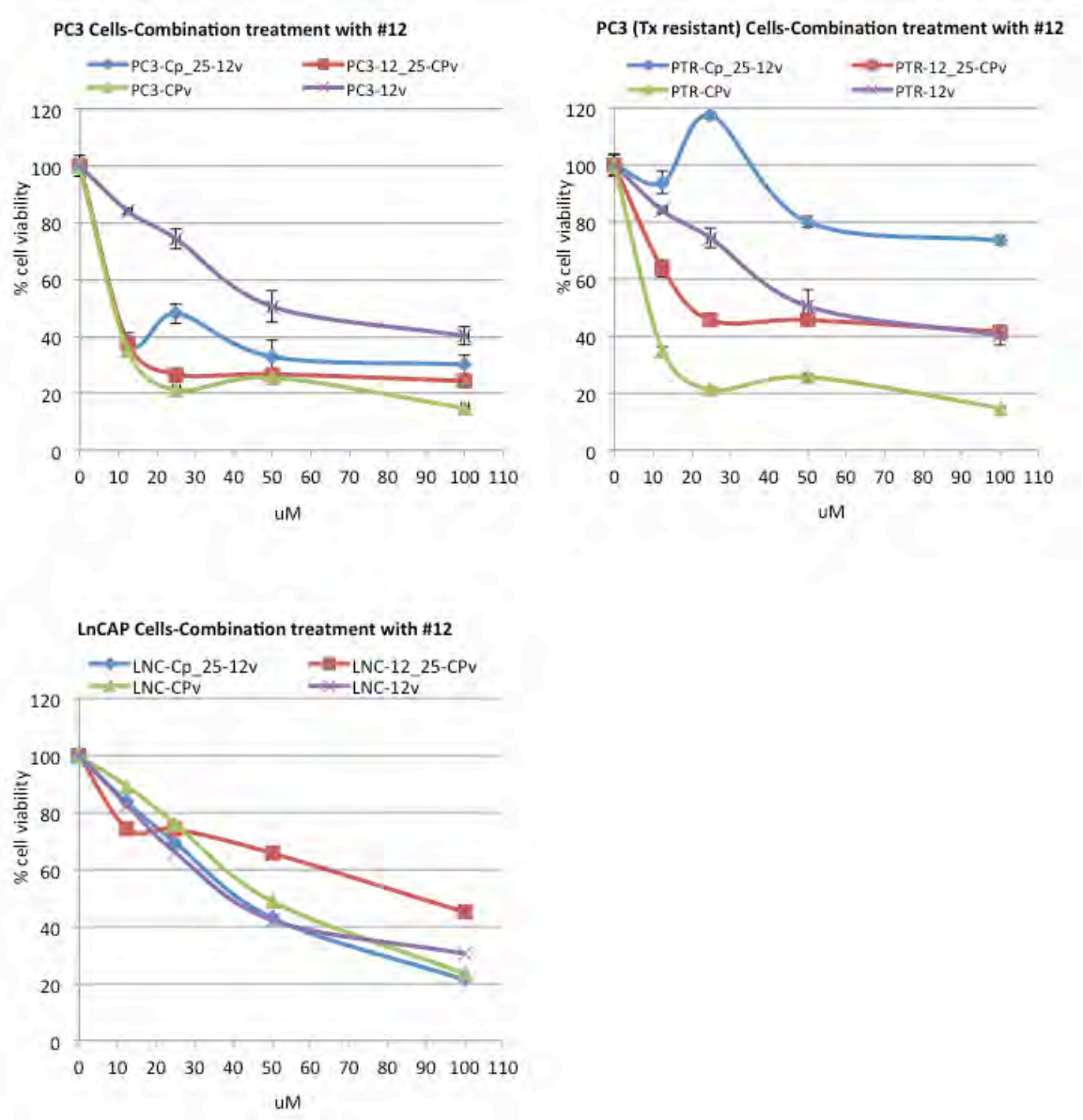

Fig. 11. Cell viability after dose-dependent combination treatment of prostate cancer cells with compound 12 and cisplatin. *Cp: cisplatin; "25" - 25 uM fixed concentration; "v" variable concentration (0-100uM).*

Figure 12 tests compound #19 in combination treatment with cisplatin. Combination treatment with fixed concentrations of #19 and increasing concentrations of cisplatin quickly demonstrates improved efficacy on cell killing. This combination treatment improves that of the individual treatments. Taxol-resistant cells, however, are less efficaciously killed, and cisplatin alone is preferred over any combination treatment. MSH2-deficient cells are sensitive to #19 alone and to combination treatment at which cisplatin is being kept at a constant concentration. In both treatments that utilize increasing concentrations of cisplatin, however, efficacy is low. It appears that the primary driver for cell killing is compound #19 in these experiments.

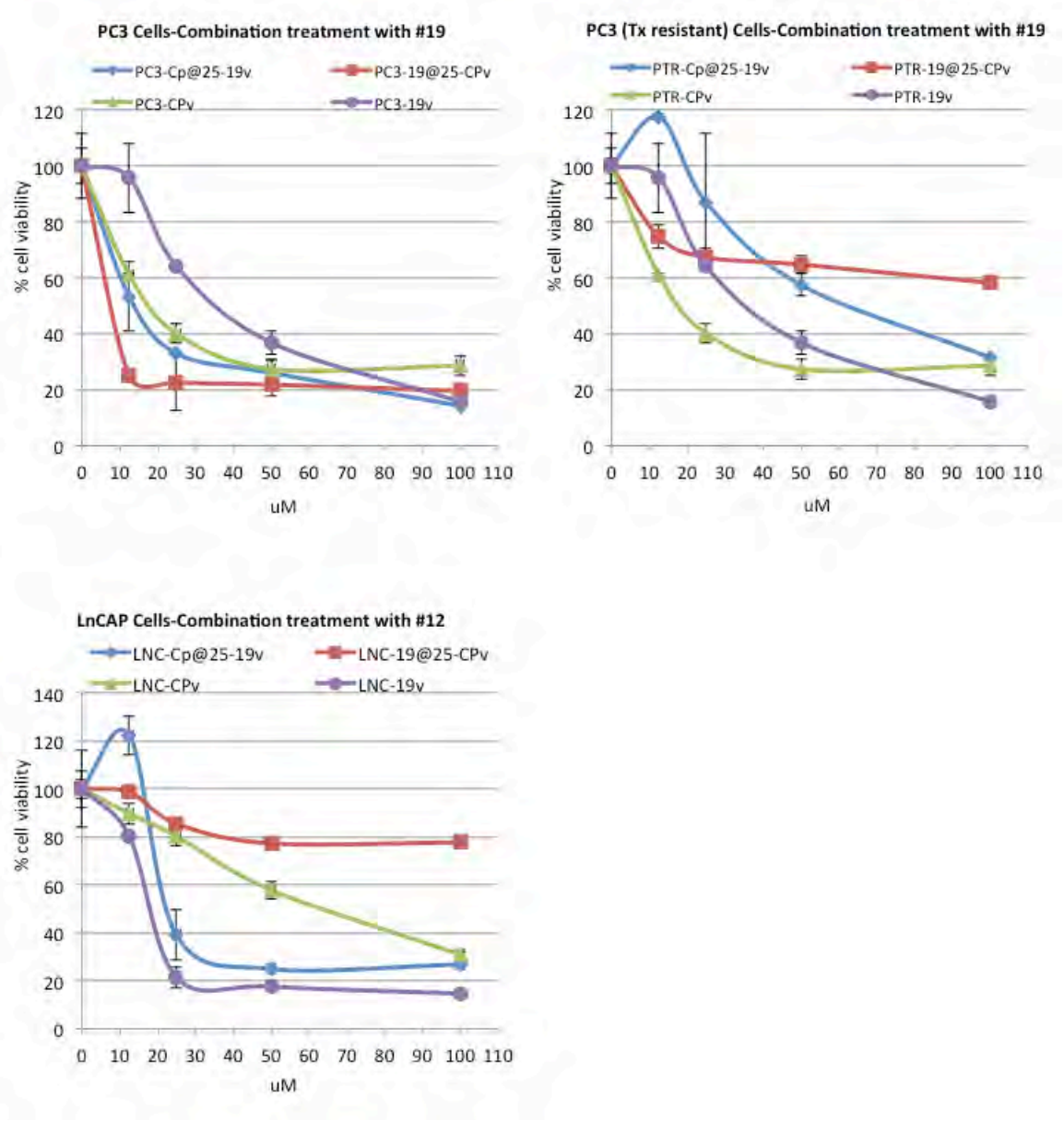

Fig. 12. Cell viability after dose-dependent combination treatment of prostate cancer cells with compound 19 and cisplatin. *Cp: cisplatin; "25" - 25 uM fixed concentration; "v" variable concentration (0-100uM).*

Figure 13 demonstrates the efficacy of compound #81 in combination treatment with cisplatin in comparison to treatment with the single compound. Compound #81 is effective in prostate cancer cells with or without taxol resistance at higher concentrations (i.e. 100 uM). The combination with cisplatin has little effect on this result in PC3 cells. No significant difference between single and combination treatment is observed in MSH2-deficient prostate cancer cells (LnCAP).

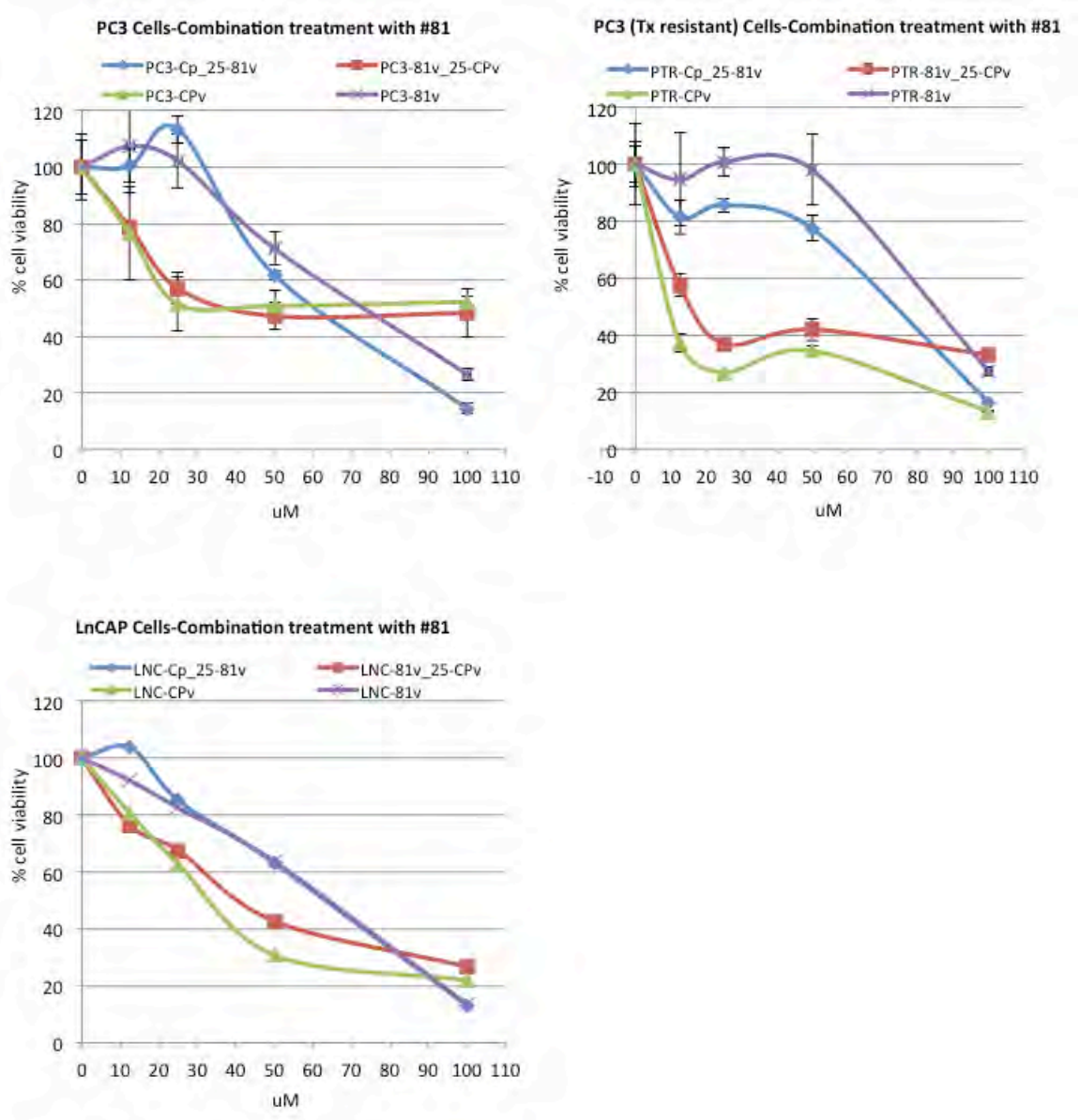

Fig. 13. Cell viability after dose-dependent combination treatment of prostate cancer cells with compound 81 and cisplatin. *Cp: cisplatin; "25" - 25 uM fixed concentration; "v" variable concentration (0-100uM).*

Figure 14 shows cell viability of prostate cancer cells after exposure to compound #84 alone and in combination with cisplatin. Combination treatment with cisplatin is more effective than treatment with #84 alone, but does not exceed it in either taxol-sensitive or resistant cells. Again, only variable amounts of cisplatin show an improvement. MSH2-deficient cells do not show a significant difference when treated in combination with cisplatin and #84, but are killed somewhat efficaciously by #84 alone.

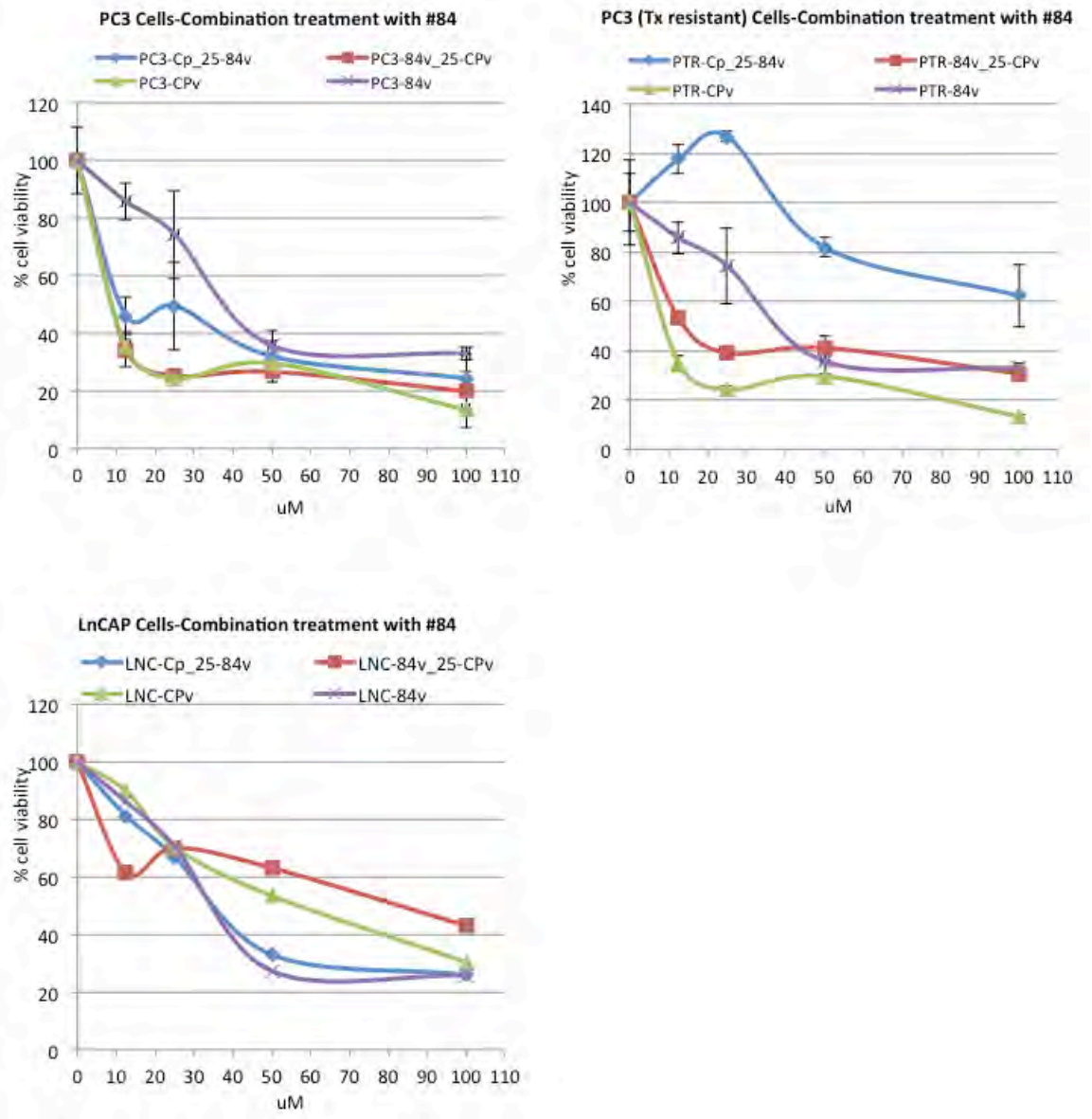

Fig. 14. Cell viability after dose-dependent combination treatment of prostate cancer cells with compound 84 and cisplatin. *Cp: cisplatin; "25" - 25 uM fixed concentration; "v" variable concentration (0-100uM).*

We next tested some of the other new compounds, e.g. 88, and use the most promising compounds against therapy-resistant prostate cancer cells and in combination therapy with taxol to determine if efficacy can be improved and whether these compounds might be an effective way to overcome resistance:

Prostate Cancer Cell Lines
Compound #84

Ra: Rescinnamine
Tx: Taxol
RaV – Tx25: Taxol at 25mM,
Rescinnamine varied

PTR: PC3 cells with taxol resistance

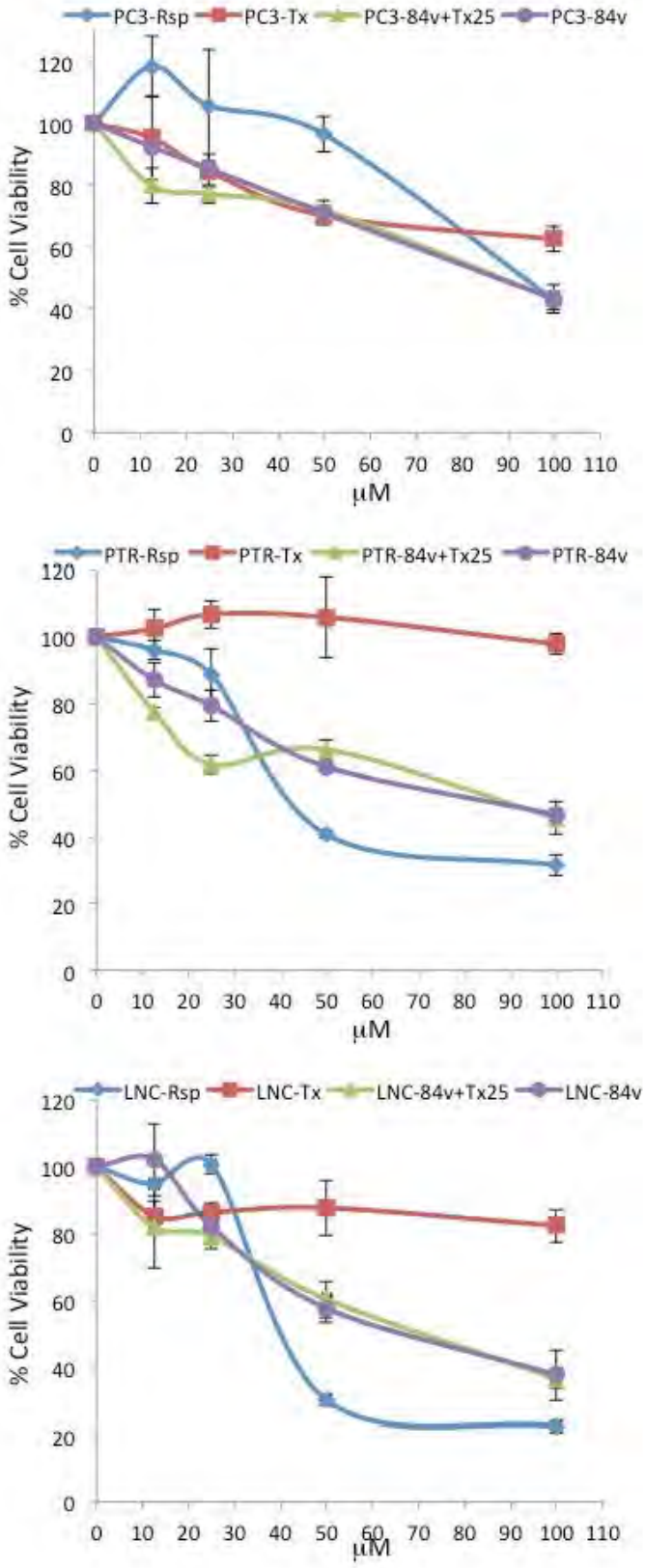

Fig. 15. Cell viability after dose-dependent combination treatment of prostate cancer cells with compound 84 and Taxol. *Tx: Taxol; "25" - 25 uM fixed concentration; "v" variable concentration (0-100uM).*

Prostate Cancer Cell Lines
Compound #88

Ra: Rescinnamine
Tx: Taxol
RaV – Tx25: Taxol at 25mM,
Rescinnamine varied

PTR: PC3 cells with taxol resistance

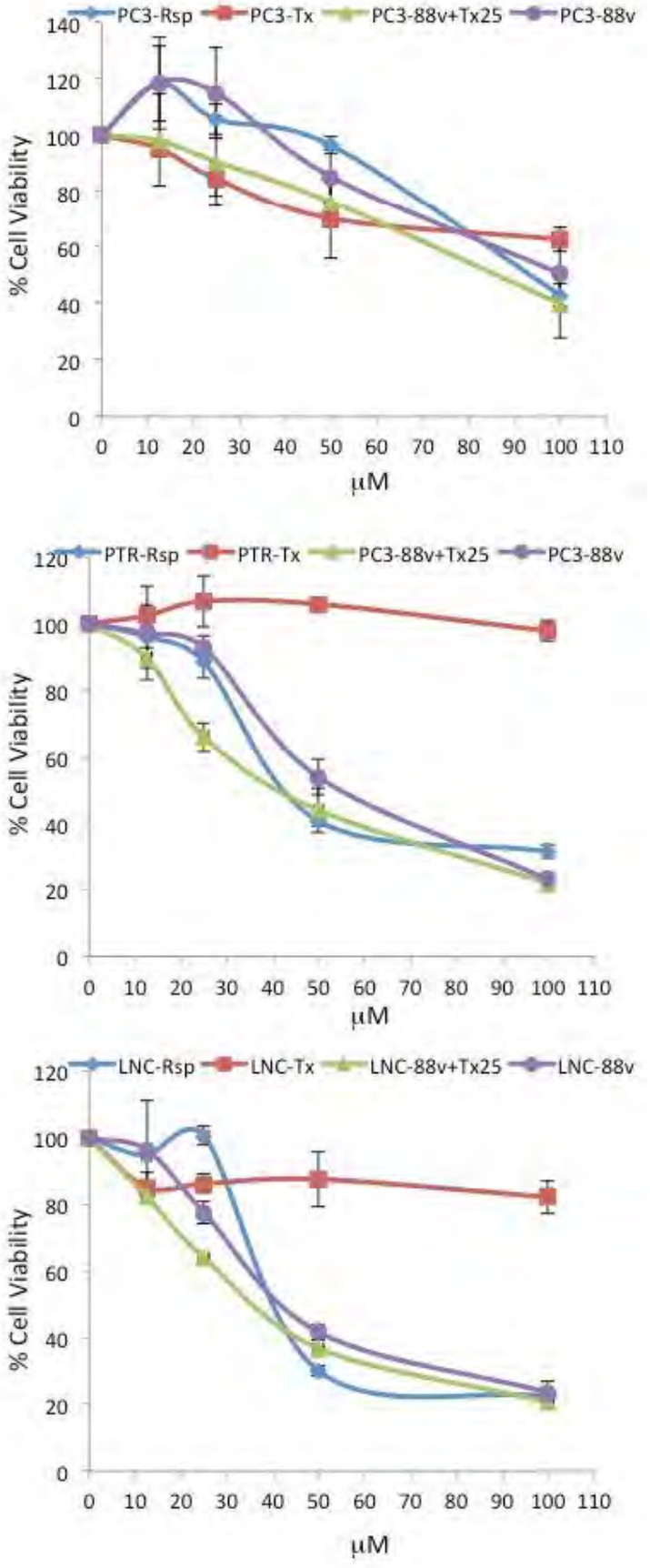

Fig. 16. Cell viability after dose-dependent combination treatment of prostate cancer cells with compound 88 and Taxol. *Tx: Taxol; "25" - 25 uM fixed concentration; "v" variable concentration (0-100uM).*

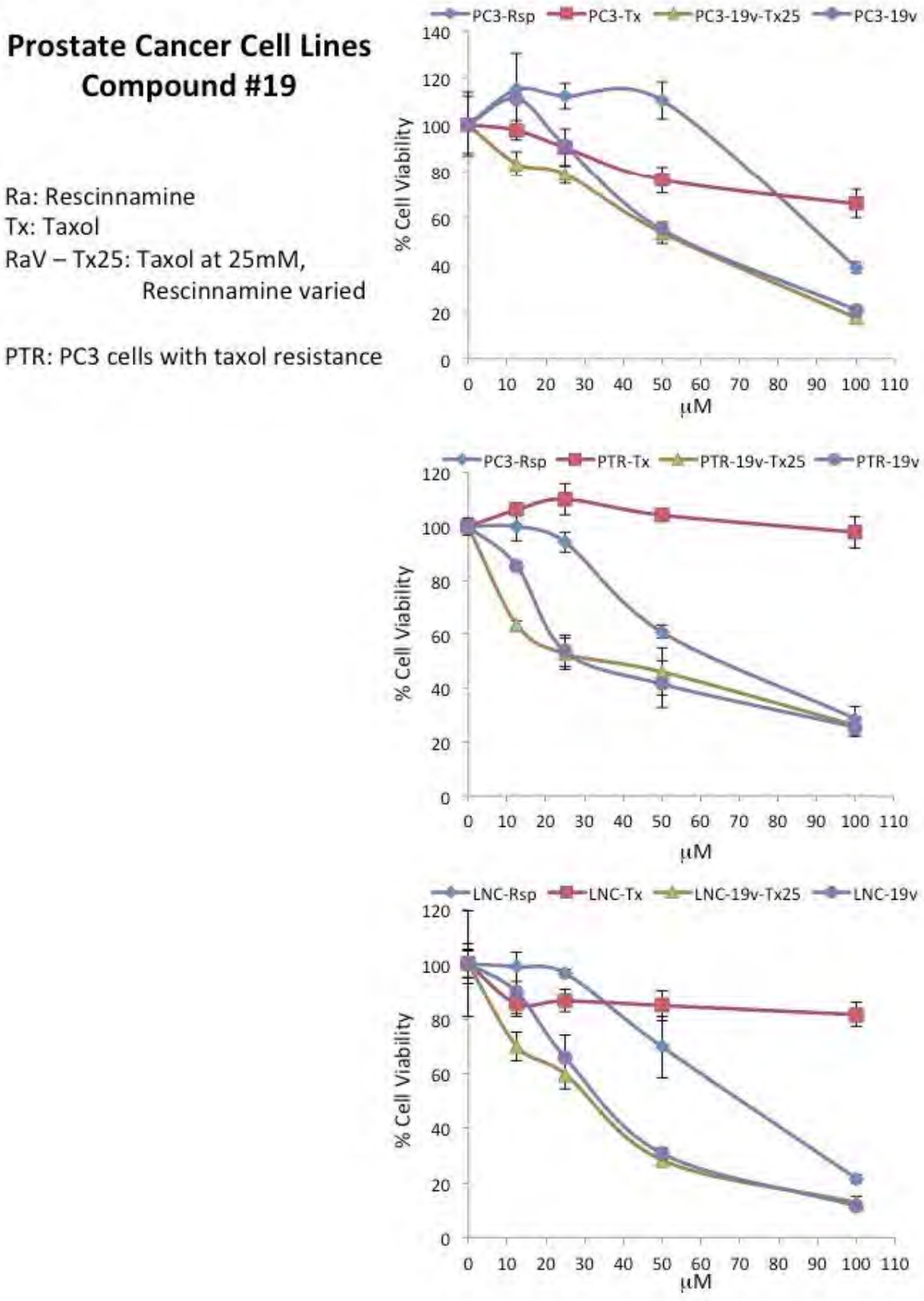

Fig. 17. Cell viability after dose-dependent combination treatment of prostate cancer cells with compound 19 and Taxol. *Tx: Taxol; "25" - 25 uM fixed concentration; "v" variable concentration (0-100uM).*

Prostate Cancer Cell Lines
Compound #12

Ra: Rescinnamine
Tx: Taxol
RaV – Tx25: Taxol at 25mM,
Rescinnamine varied

PTR: PC3 cells with taxol resistance

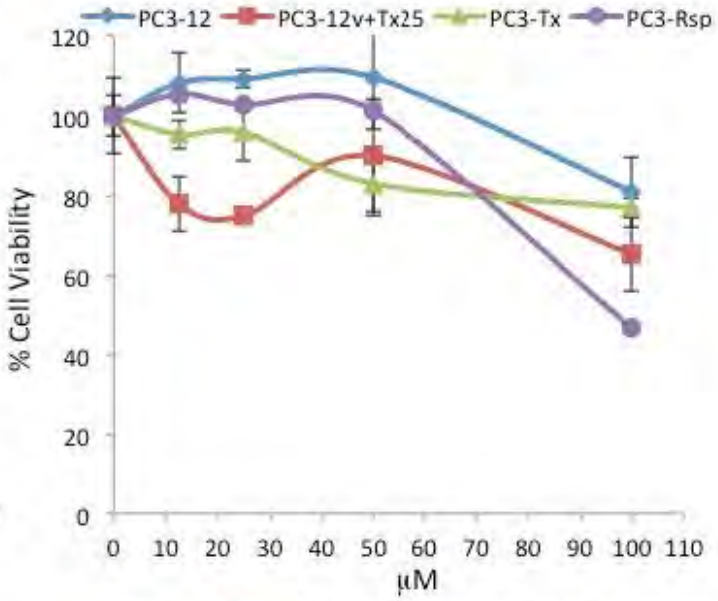

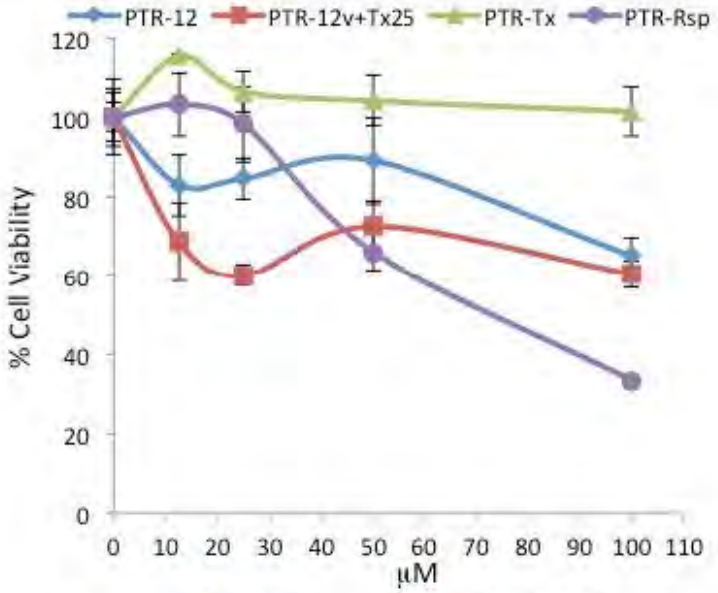

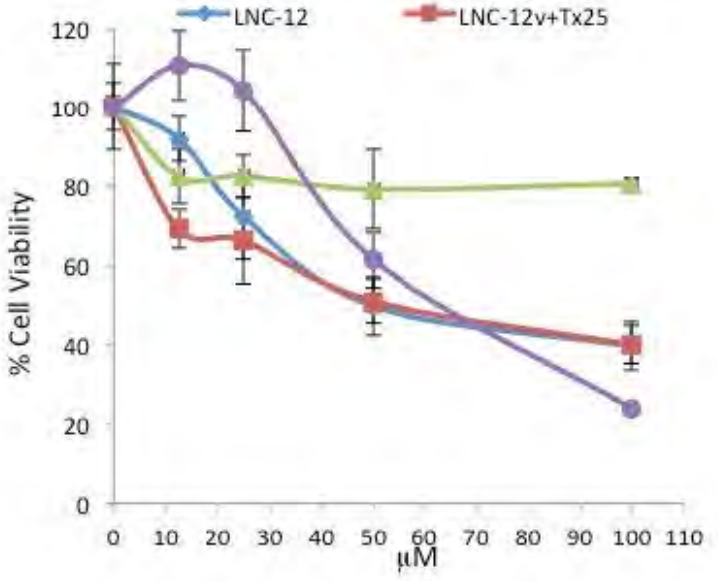

Fig. 18. Cell viability after dose-dependent combination treatment of prostate cancer cells with compound 12 and Taxol. *Tx: Taxol; "25" - 25 uM fixed concentration; "v" variable concentration (0-100uM).*

Prostate Cancer Cell Lines
Compound #81

Ra: Rescinnamine
Tx: Taxol
RaV – Tx25: Taxol at 25mM,
Rescinnamine varied

PTR: PC3 cells with taxol resistance

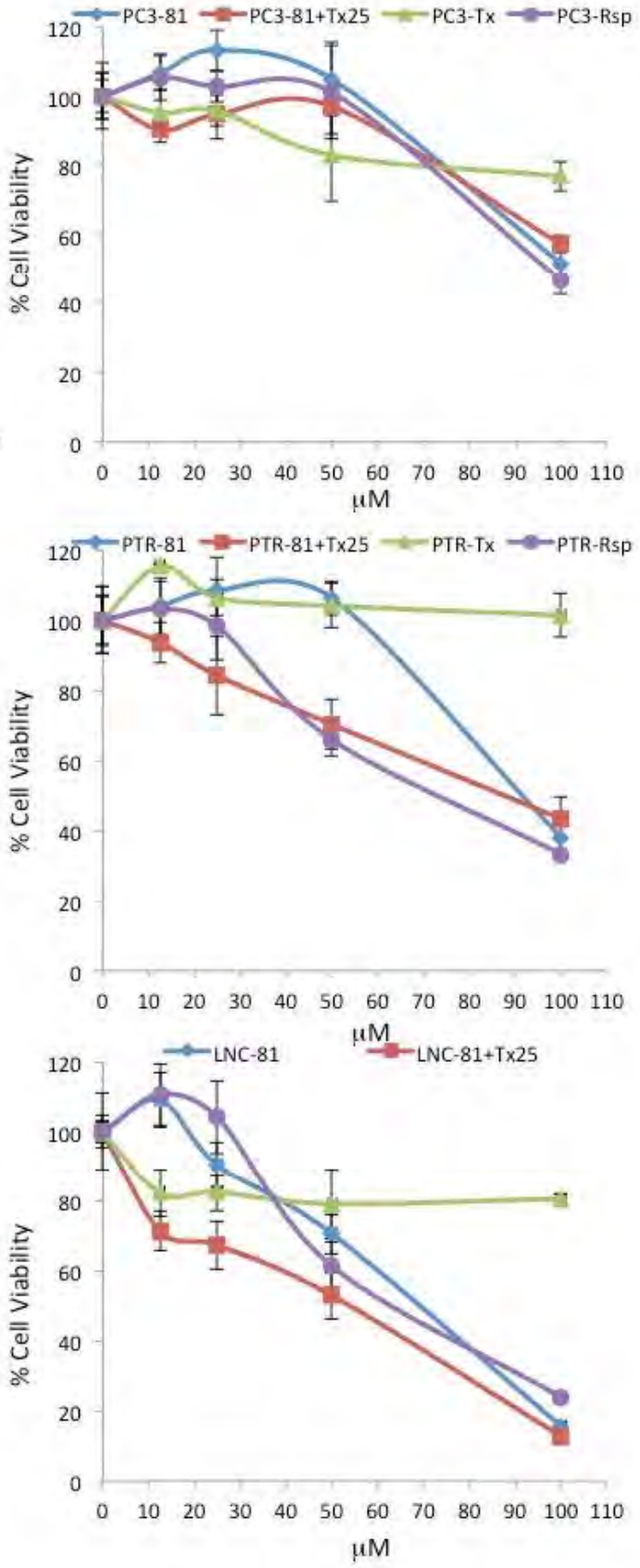

Fig. 19. Cell viability after dose-dependent combination treatment of prostate cancer cells with compound 81 and Taxol. *Tx: Taxol; "25" - 25 uM fixed concentration; "v" variable concentration (0-100uM).*

Results from these combination studies indicate that compounds 84, 88, 19 and 12 induce cell death in taxol resistant PC3 cells, with 19 being most effective. Compound #81 has a cell killing effect on taxol resistant PC3 cells that appears to be improved in the presence of taxol, while the efficacy of none of the other compounds appears to be improved by combination treatment.
Combination with taxol does not improve the efficacy of any of these new compounds in LnCAP cells, though all of these compounds show efficacy again LnCAPs.

Determine induction of pro-apoptotic proteins
As a control, we first performed assays on the induction of pro-apoptotic proteins with compounds known to induce or not induce the targeted response in PC3 prostatic cancer cells:

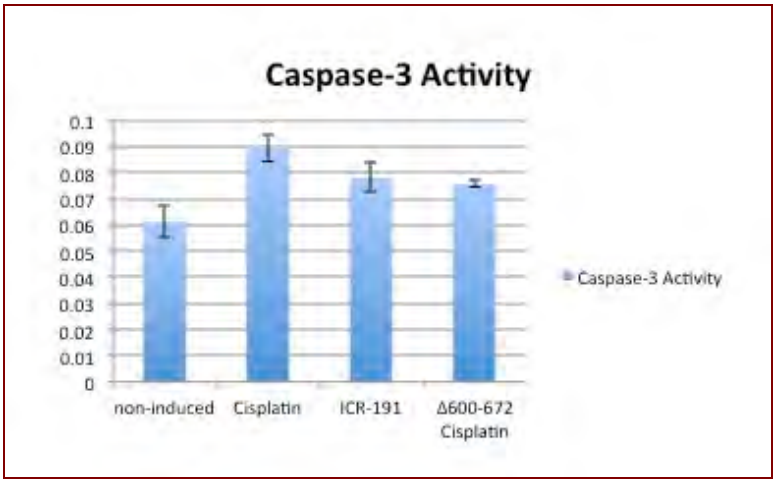

Fig. 20. Induction of caspase-3 as evidence of apoptotic activity in PC3 cells. *Cells were exposed to cisplatin and the frameshift inducer ICR-191. Delta 600-672 contains a deletion mutation in MSH2 that avoids nuclear import as part of the damage response.*

Cisplatin showed some induction of caspase-3 activity in PC3 cells. This assay will be repeated once the best new compounds have been singled out.

We added an additional experiment to our list that looked at the mechanism of MSH2 involvement in apoptotic response. Our previous observations suggested that MSH2-mediated apoptosis required nuclear import of the protein upon exposure to certain cytotoxins or genotoxins. We determined here if Cisplatin or ICR-191 induced such nuclear influx in PC3 prostatic cells:

We have begun apoptotic measurements of the new compounds, using laser-scanning confocal microscopy and a newly acquired flow cytometer. For the confocal microscopy experiments, cells were plated on a tissue coated cover slip, incubated under standard conditions in full media for 24 hours, and then treated with resinnamine analogs for 3 or 6 hours in the presence of a caspase detection substrate. Using Zeiss LSM 710 confocal microscope, were able to image the cells (**Figure 21**) and determine the percentage of cells with an increase in caspase activity at specific timepoints. The data are summarized in **table 3**.

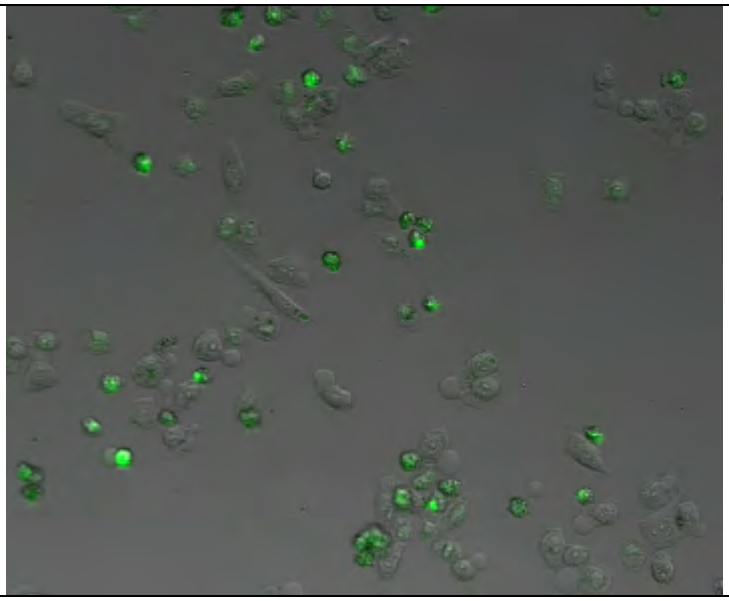

Fig. 21 Caspase activity in PC3 cells treated with analog 88.
Cells were plated and cultured on a tissue culture treated coverslip for 24 hours. Next, analogs were added to the culture media along with a caspase detection substrate which became fluorescent in the presence of caspase 3 and 7.

Results are shown in **Table 3**.

	Time (min)	88		84		81		19		12	
		Avg	Stdev	Avg	Stdev	Avg	Stdev	Avg	Stdev	Avg	Stdev
PC3	180	33.9	9.3								
	360	48.0	6.1	4.6	1.1	8.3	2.6	3.8	1.0	1.3	0.6
PTR	180	18.1	5.8								
	360	58.4	9.7	0.8	0.2	7.2	0.7	4.2	3.2		
LnCAP	180	76.8	3.0	10.4	3.9	6.0	0.5	11.5	0.3	2.8	0.1

The table shows average percentage of cells showing significant caspase 3 activity. Compound 88 shows by far the strongest induction of caspase 3 activity in any of the prostate cancer cell lines.

We were able to use flow cytometry to analyze cells treated under identical conditions to those in the confocal experiments. Hence, flow cytometry was used to detect the presence of Caspase 3 and 7 in PC3, PTR, and LnCap cells exposed to analogs of Rescinnamine. For each cell line, a control group was incubated in identical conditions but in the absence of analogs and used to establish a baseline for Caspase 3,7 activity. For the PC3 and PTR cell lines, the concentration of Rescinnamine analog was 200 mM and the time of exposure was 2 hours. For the LnCap cell line, it was necessary to use a lower concentration (50 mM) of analogs and a shorter time of incubation (1 hour) as these cells entered apoptosis more quickly and at much lower doses.

For each cell line, 20,000 cells were submitted to flow cytometry for fluorescence detection and analysis. These data are shown in **Table 4.**

	Treatment Group	M1-Low	M2-Med	M3-High
PC3	Control	71.9	18	1
	L+88	0.7	44.1	43.3
	L+84	3.6	71.8	6.8
	L+81	1.4	67.8	21.4
	L+19	3.7	42.7	33.8
	L+12	36.6	36.5	2.8
	L+Rsp	53	33.6	0.9
PTR	Control	76.5	4.8	1.9
	L+88	0.2	68.8	21.4
	L+84	5.1	60.2	10.5
	L+81	3.8	56.9	6.8
	L+19	6.3	60	2.7
	L+12	35.6	23.9	3.1
	L+Rsp	72.9	4.9	5.6
LnCap	Control	47.7	15	17.9
	L+88	5.7	19.1	62.4
	L+84	8.9	30.8	35.6
	L+81	20.4	52.3	6.4
	L+19	19.8	55.2	4.8
	L+12	9.6	53.5	10
	L+Rsp	4.7	63.1	11.6

Table 4 Flow cytometry data for PCR, PTR, and LnCap cells.

Figure 22 shows the fluorescent intensities in PC3 cells exposed to Rescinnamine analogs for 2 hours.

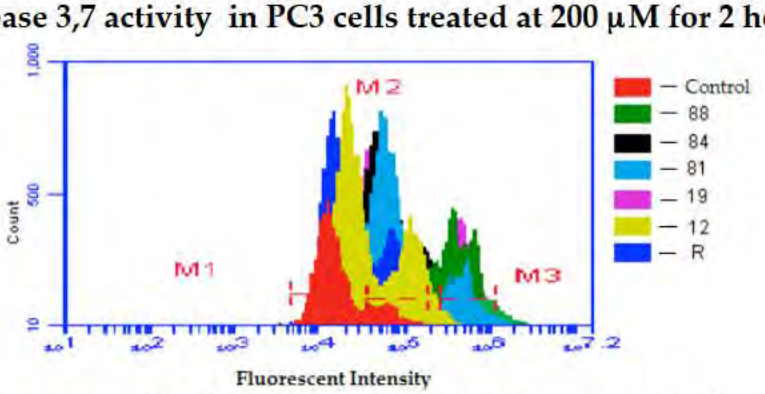

Figure 22. Fluorescent intensity distributions in PC3 cells exposed to Rescinnamine analogs. *Numerical data (for PC3 cells) from Table 3 is represented graphically, showing the distributions of fluorescent intensities within the three cell populations for each treatment group.*

From this image, it can be seen that analog 88 induces apoptosis more strongly than the other analogs. The fluorescent intensity, in each cell, is proportional to the concentration of Caspase 3 and 7. As such, an increase in caspase concentration results in an increase in fluorescent intensity.

In each case, three distinct populations of cells with different fluorescent intensities were observed; low, medium, and high (**Fig. 23**.)

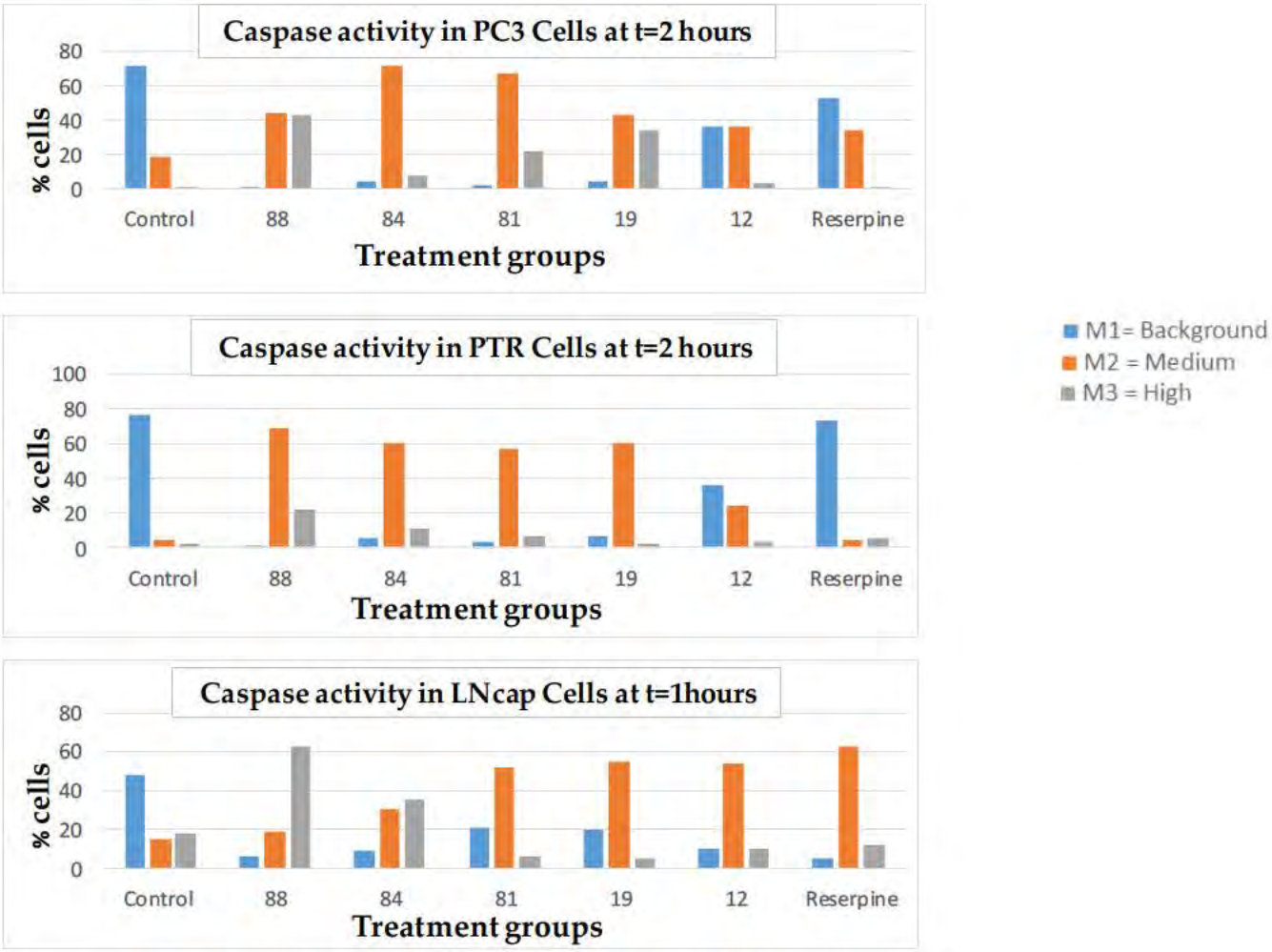

Figure 23. Rescinnamine induced caspase 3,7 activity in PC3, PTR, and LnCap cells*. These bar graphs show the percentage of cells within each of the three distinct populations for PC3, PTR, and LnCap cells after exposure to Rescinnamine analogs.*

Since an increase in fluorescence indicates an increase in caspase concentration, the data provides us insight into how quickly each analog induces apoptosis. In Fig. 23, untreated cells show background fluorescence due to baseline levels of caspase activity not induced by analog treatment. This population of cells, which we gate as **M1,** have the lowest levels of fluorescence and in turn the lowest concentration of caspase. The other two populations of cells, **M2** and **M3**, have higher levels of fluorescence intensities by at order of magnitude of a logarithmic scale. This difference indicates significant differences in the concentrations of caspase. These data all show that analog 88 consistently induces apoptosis more strongly than the other analogs.

We begun to test if treatment changes the subcellular localization of mismatch repair proteins and thereby can affect response to chemotherapeutic agents (**Fig. 24**)

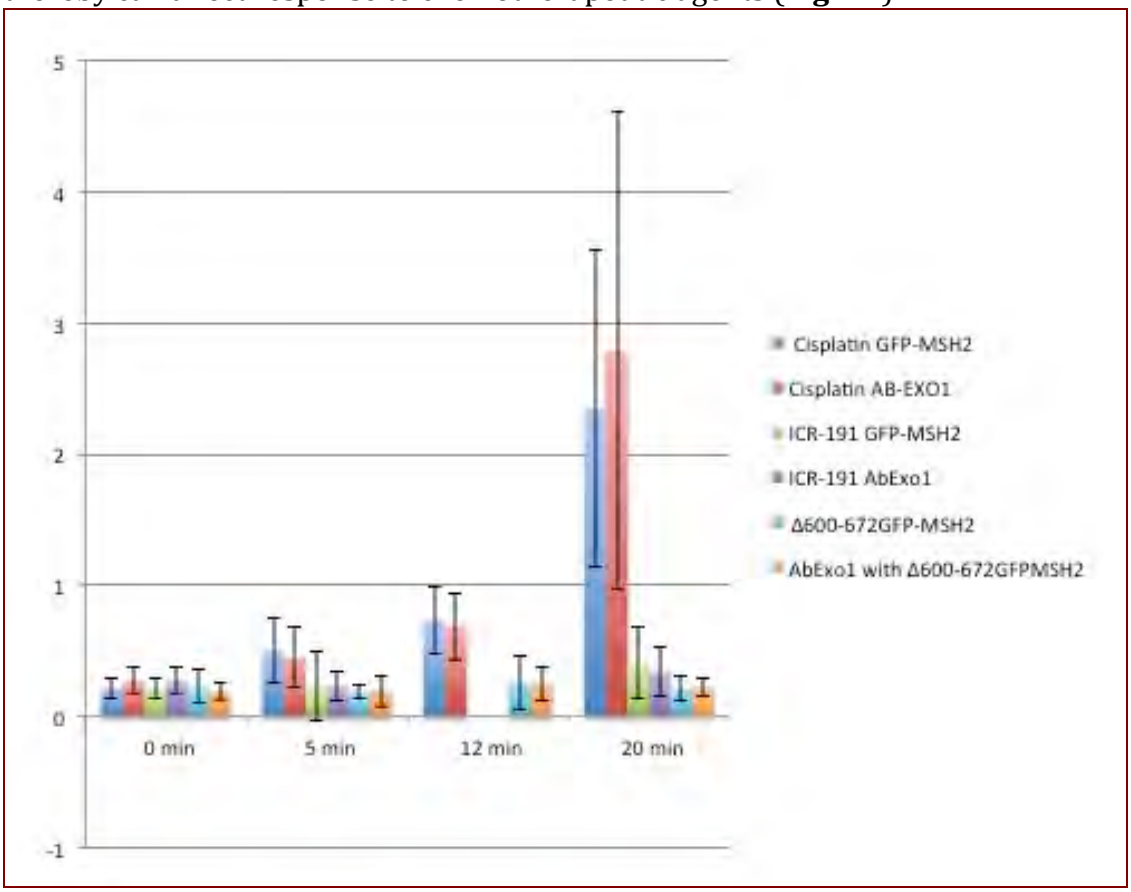

Fig. 24. Nuclear import of MSH2 and Exo1 upon treatment with cisplatin and ICR-191, respectively.

We demonstrated that only cisplatin induced nuclear influx of MSH2 upon treatment. It remains to be determined if any of our new compounds induce a similar response.

Task 2: To determine rescinnamine-induced tumor growth inhibition in hormone-refractory tumors *in vivo*

Together with Washington Biotechniques, the following experiments were performed:

PROCEDURES:

A. Preparation of Human Cancer Cell Line.

1. Thaw out frozen (liquid nitrogen) aliquot of PC3 cells (ATCC: human prostate adenocarcinoma).
2. Disperse into 75 cm^2 flask containing RPMI 1640 media supplemented with 10% fetal bovine calf serum (FBS) and incubate at 37°C in humidified atmosphere of 5% CO_2.
3. As cells become 90% confluent, expand cultures to 225 cm^2 flasks.
    a) Supplement or renew culture media as needed.
4. Continue to expand culture until sufficient cells are available for injections. Cells are harvested by trypsinization, washed and re-suspended to a concentration optimal for implantation.

5. Cells required:

B. Establishment of Tumors.

1. Receive (SOP 1910, SOP 1920) 90 male athymic nude mice (5-6 weeks) and house in filter-topped autoclaved cages supplied with autoclaved bedding.
2. Animal handling procedures are under laminar flow hood.
3. Implantation:

    a) Mice are ear-tagged (SOP 810) for individual identification.
    b) Record weight of each mouse.
    c) Inject cancer cells subcutaneously (SOP 1610) in right front flank with 5 million cells in 0.1 ml PBS with 10% matrigel.
    d) Injection of 90 mice; total cells required 450 million.

4. Staging:

    a) Measure tumor dimensions using electronic calipers.
    b) Record tumor measurements every Monday and Thursday until tumor volumes are in a range 80-150 mm^3.
    c) To reduce variability in measurements, tumor dimensions for a study are taken by one technician throughout the Study.

C. Treatment Regimen:

a) Record mouse weights.
b) Record tumor size measurements.
c) Sort animals into 12 treatment groups of 6 mice per group based upon tumor size. Mice are selected and distributed among groups so as to have a similar mean tumor size (within 80-150 mm^3) for each group.
d) Start dosing regimen with intraperitoneal dosing (IP: SOP 1650) once daily (QD) for 14 days.

TABLE5: GROUP TREATMENTS

Group	Group Name	Dose (mg/kg/d)	#Animals	ROA	Dose Schedule
1	Vehicle 1	0	6	IP	QD, 14 days
2	Rescinnamine	1	6	IP	" "
3	" "	3	6	IP	" "
4	" "	5	6	IP	" "
5	Vehicle 2	0	6	IP	" "
6	Paclitaxel	2.5	6	IP	" "

7	"	"	5.0	6	IP	"	"
8	"	"	10.0	6	IP	"	"
9	Vehicle 3		0	6	IP	"	"
10	Resc + drug*		1	6	IP	"	"
11	"	"	3	6	IP	"	"
12	"	"	5	6	IP	"	"

IP = intraperitoneal injection (SOP 1650)

*Drug = paclitaxel at fixed concentration 5 mg/kg and rescinnamine varied as indicated

D. Monitoring.

a) Record mouse weights twice weekly, Monday and Thursday.
b) Daily health check for any signs of clinical distress. Any significant clinical sign will be recorded and discussed with Sponsor.
c) Record tumor measurements twice weekly, Monday and Thursday.
d) Dose mice following schedule in TABLE 5.
e) Calculate tumor volumes using formula:

Tumor Volume = (Length x Width x Width)/2

f) For each date of measurements: Tabulate tumor measurements, calculate mean tumor volume and body weight for each group and standard deviation. Graph mean tumor volumes and body weight changes together with variability for each group against time from initial dose.

E. Termination:

a) Euthanize mice (SOP 1720) and collect tumors tissue from each animal and weigh. Preserve tumors in 10% neutral buffered formalin to be available for histopathology if required. Histopathology is available as an optional item to be ordered separately.

b) Tumor growth inhibition is calculated for each test group and control group: T/C.

Results:

Controls:

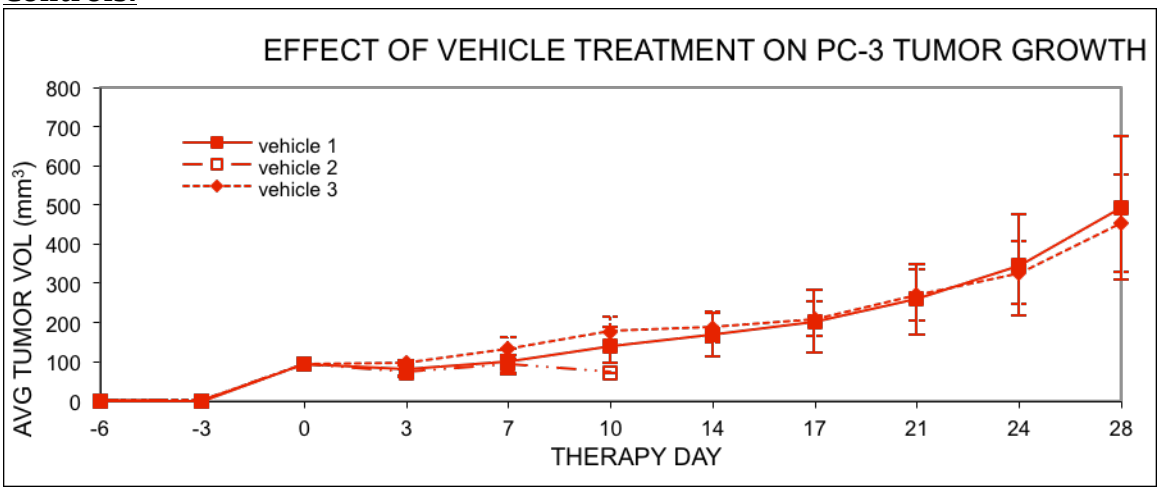

Fig.25. Determination of the effect of vehicle treatment on PC-3 tumor growth

As seen in Fig. 25, the solvent does not affect the growth of tumors, which grow, as expected. The mice receiving vehicle 2 (Cremaphor/50% ethanol) were found dead at day 10. It is unclear if the vehicle was toxic, or they died of other causes.

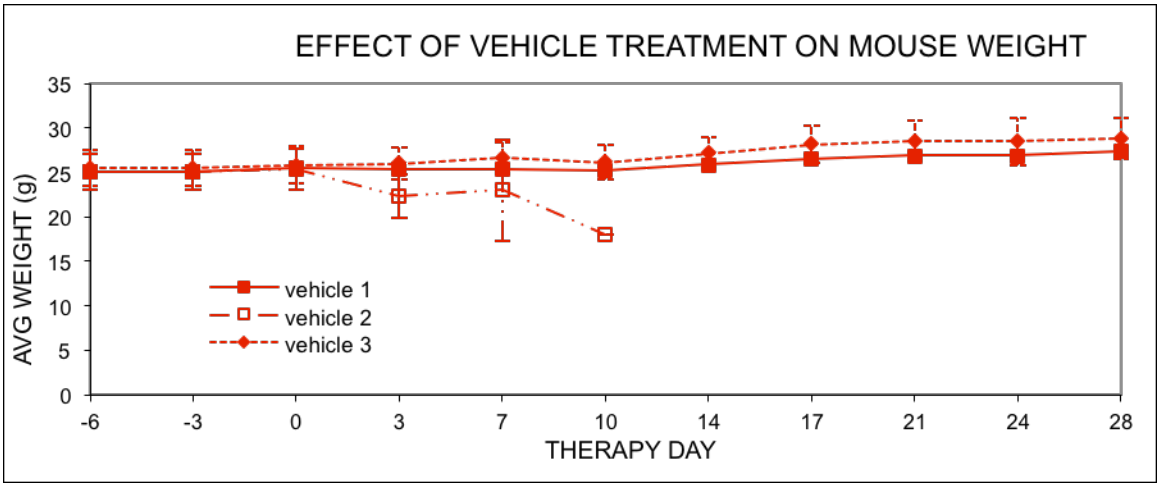

Fig. 26. Effect of vehicle treatment on mouse weight

Apart from the uncertain effects seen with vehicle 2, vehicle treatment did not show a noticeably effect on mouse weight.

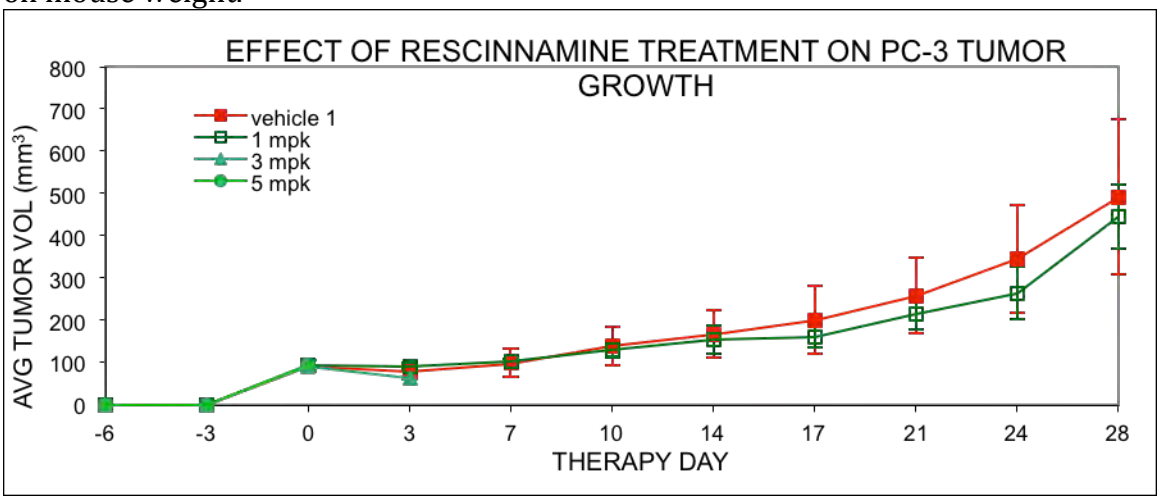

Fig. 27. Effect of rescinnamine on PC-3 xenografts.

As seen in Fig. 27, rescinnamine had a very mild, not statistically significant effect on tumor growth. At higher concentrations, mice were found to experience severe signs of hypotension and were eventually euthanized. Necropsy suggested inflammations to the intestines, potential effects to liver and lungs. Lower concentrations of rescinnamine did not affect the weight of mice.

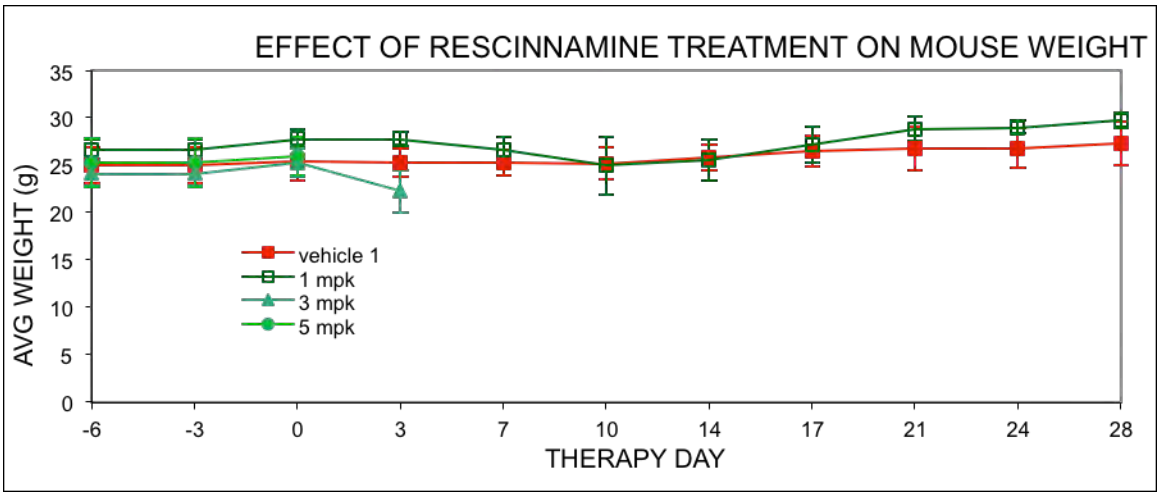

Fig. 28. Effect of rescinnamine on mouse weight.

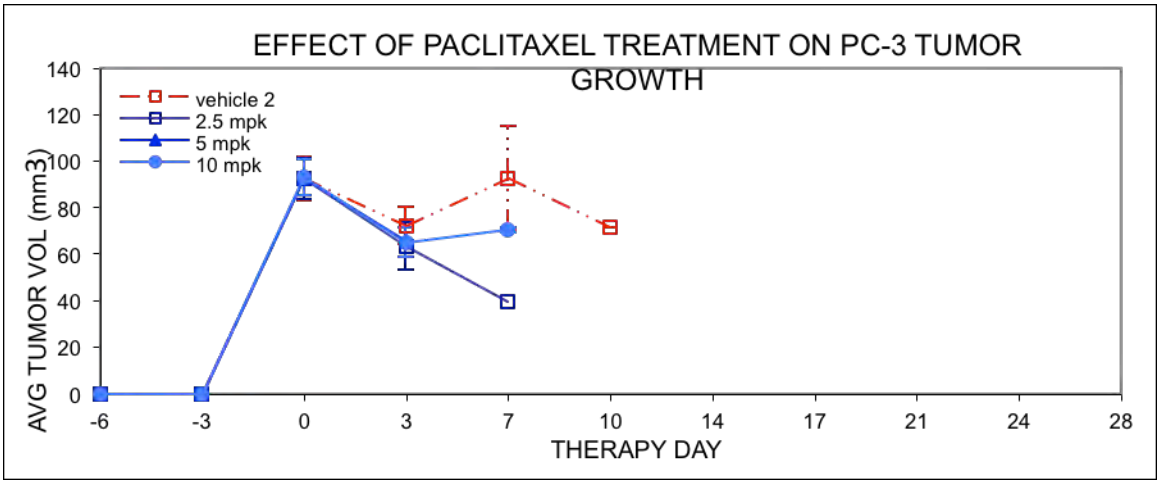

Fig. 29. Treatment of PC3 tumors with paclitaxel

As seen in Fig. 29, treatment with paclitaxel in vehicle 2 was not well tolerated by the mice who were euthanized by day 10. Given previous results with vehicle alone (see above) and the fact that paclitaxel concentrations were those described in the literature before, this may reflect toxicity of the vehicle.

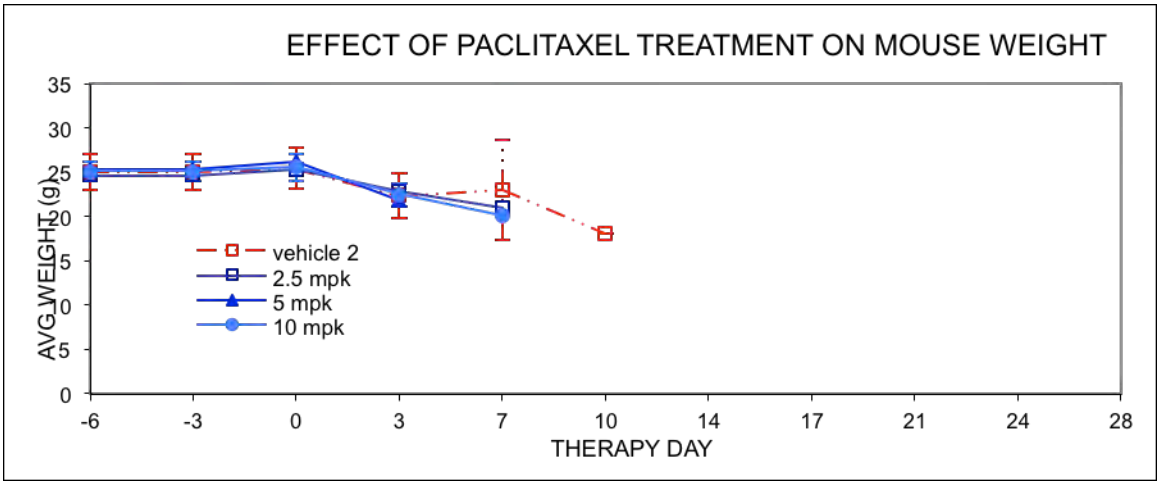

Fig. 30. Effect of paclitaxel and vehicle on mouse weight.

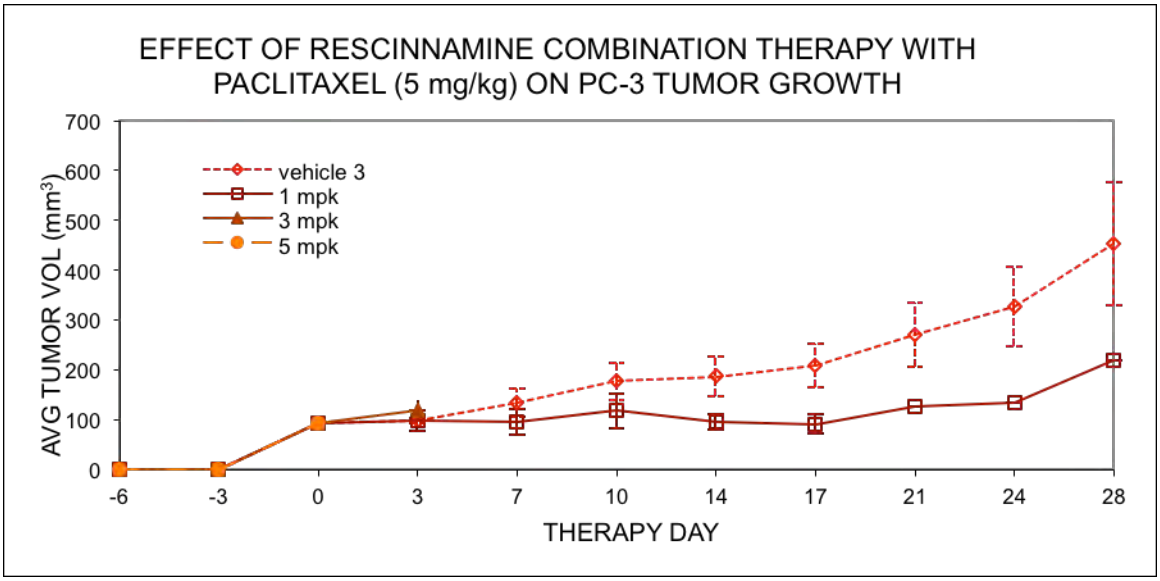

Fig. 31. Effect of rescinnamine and paclitaxel together on PC3 growth

As shown in Fig. 31, the combination of rescinnamine (lowest concentration) with paclitaxel has a significant effect on tumor growth. Since the paclitaxel only treatment had to be abandoned early, it is unclear if this represents a significant improvement over paclitaxel alone. After keeping the tumor at the same size for about 3 week, the last measurement seems to indicate that tumors would continue growing after the initial hold. Combination treatment caused a reversible and temporary lowering of body weight.

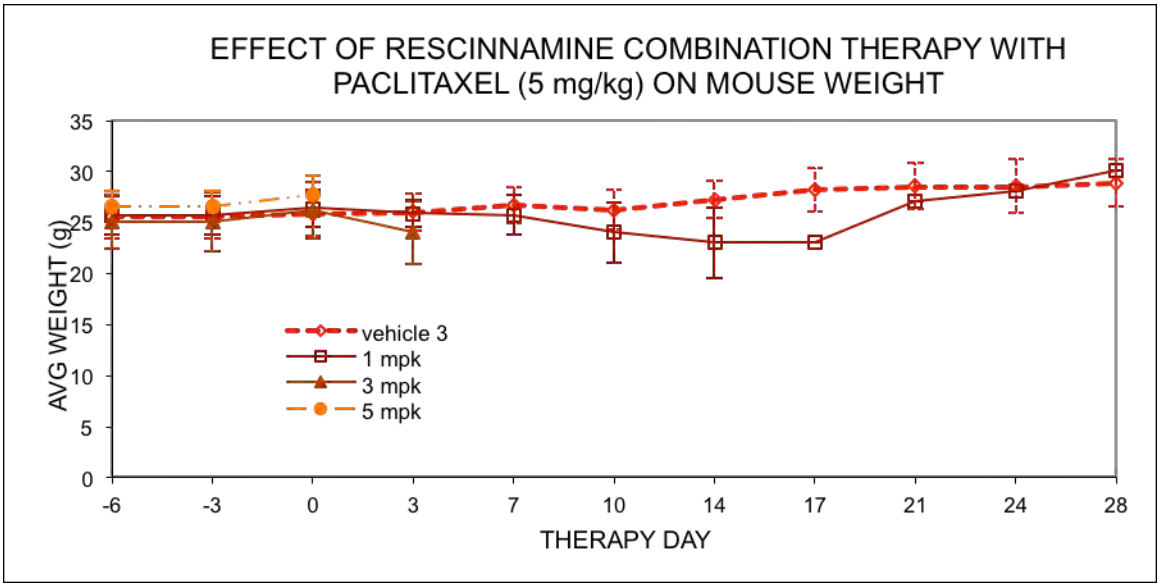

Fig. 30. Mouse weight after treatment with rescinnamine and paclitaxel

5. Conclusions

Given our results, combined with those above, we conclude that rescinnamine itself would only be effective, if given with another drug that counteracts the hypotensive effect of the drug. Since such combination treatment would have additional problems, we decided to go with our other solution to modify rescinnamine in an effort to minimize its hypotensive activity and maximize its tumor inhibitory function. We have performed computational modeling and chemical synthesis of new rescinnamine analogs with the goal to identify such that might be effective against prostate cancer cells. At least two new compounds were found to be effective in cell culture. These have been tested for efficacy in an MSH2-dependent and independent environment, in prostate cancer and in combination treatment with cisplatin. Most importantly, combination treatment with taxol shows no added advantage over single treatment. Overall, our data suggest that new compound #88 is more efficacious than any other rescinnamine-like compound and appears to be effective in taxol-resistant prostate cancer cells. Compound #88 would now be ready for animal testing to determine efficacy against tumorigenesis.

6. Publications

The following manuscripts were supported by this project:

Jarzen, J., Diamanduros, A., and **K. Scarpinato** (2013). Mismatch repair proteins in recurrent prostate cancer, *Adv. Clin. Chem.* 60, 65.

AbdelHafez, E. M.N., Diamanduros, A., Bean, J.H., Zielke, K., Crowe, B., Vasilyeva, A., Clodfelter, J.E., Aly, P.M., Abuo-Rahma, G.E.D.A.A., **Scarpinato, K.D**.*, Salsbury, F.R.*, King, S.B.* (2013). Improving rescinnamine as an inducer of MSH2-dependent apoptosis in cancer treatment. Mol. Cancer Biol. 1, 1. (* corresponding authors)

We are planning on submitting another manuscript summarizing the data obtained with new rescinnamine analogs.

7. Inventions, Patents and Licenses

The results from this research are part of a patent disclosure, US patent no. 14/193,371.

8. Reportable Outcomes

- Rescinnamine has been tested against all prostate cancer cell lines, and found not to be highly effective against prostate cancer
- We have performed computational docking and chemical synthesis to identify rescinnamine analogs that may have higher efficacy and eventually less hypotensive activity
- 17 new compounds were synthesized and tested for their effects on cell viability
- 3 of these compounds that showed best activity in pre-tests were tested against prostate cancer cells
- 2 of these compounds show significant activity against prostate cancer (#81, 88)
- Combination treatment with cisplatin or taxol does not show a clear benefit of this combination
- new compound #88 shows high cell killing efficacy in prostate cancer cell lines, including taxol resistant cells that stems from the induction of apoptosis

9. References

Hoshino, Y., Okuno, M., Kawamura, E., Honda, K., Inoue, S. (2009). Base-mediated rearrangement of free aromatic hydroxamic acids (ArCO-NHOH) to anilines. Chem. Commun. 2281–2283.

Morris, G. M., Huey, R., Lindstrom, W., Sanner, M. F., Belew, R. K., Goodsell, D. S. and Olson, A. J. (2009) Autodock4 and AutoDockTools4: automated docking with selective receptor flexiblity. J. Computational Chemistry, 16, 2785-91.

Negureanu, L., and Salsbury Jr, F. R (2012). Insights into protein - DNA interactions, stability and allosteric communications: a computational study of mutSα-DNA recognition complexes. J Biomol Struct Dyn.29, 757-76.

Patel, B.A., Ziegler, C.B., Cortese, N.A., Plevyak, J.E., Zebovitz, T.C., Terpko, M., Heck, R.F. (1977). Palladium-catalyzed vinylic substitution reactions with carboxylic acid derivatives. J. Org. Chem. 42, 3903–3907.

Pearce, H.L., Safa, A.R., Bach, N.J., Winter, M.A., Cirtain, M.C., Beck, W.T. (1989). Essential features of the P-glycoprotein pharmacophore as defined by a series of reserpine analogs that modulate multidrug resistance. Proc. Natl. Acad. Sci. U.S.A. 86, 5128–5132.

Salsbury Jr., F.R. (2010) Molecular dynamics simulations of protein dynamics and their relevance to drug discovery. Current opinion in pharmacology. 10, 738-44.

Vasilyeva, A., Clodfelter, J.E., Rector, B., Hollis, T., Scarpinato, K.D., and Salsbury Jr., F.R. (2009). Small molecule induction of MSH2-dependent cell death suggests a vital role of mismatch repair proteins in cell death. DNA Repair 8, 103-113.

Vasilyeva, A., Clodfelter, J.E., Gorczynski, M.J., Gerardi, A. R., King, S. B., Salsbury, F., and Scarpinato, K.D. (2010). Parameters of reserpine analogs that induce MSH2/MSH6-dependent cytotoxic response. J. Nucl. Acids 2010, 1-13.

Ziegler, C.B., Heck, R.F. (1978). Palladium-catalyzed vinylic substitution with highly activated aryl halides. J. Org. Chem. 43, 2941–2946.